Exploring astro-neutrinos and WIMPs through nuclear recoils

Dimitrios K. Papoulias

University of Ioannina, Greece

RCNP NEWS colloquium, Osaka University, Japan

Ευρωπαϊκή Ένωση
European Social Fund

Operational Programme
Human Resources Development,
Education and Lifelong Learning

Co-financed by Greece and the European Union

ΕΣΠΑ 2014-2020
ανάπτυξη - εργασία - αλληλεγγύη

Outline

1. CEvNS in the Standard Model
   - Nuclear form factors
2. Non-standard interactions(NSIs)
   - light and heavy mediators
3. Electromagnetic neutrino vertex
   - Transition Magnetic Moments (TMMs)
   - impact of CP violating phases
   - comparison with Borexino
4. Sterile neutrinos and Non-Unitarity (NU)
   - sensitivity on the mixing parameters
   - sensitivity on the NU parameters
5. WIMP-nucleus scattering
   - neutrino backgrounds
   - neutrino floor
6. Summary

What is CEνNS ?

CEνNS: Coherent elastic neutrino nucleus scattering

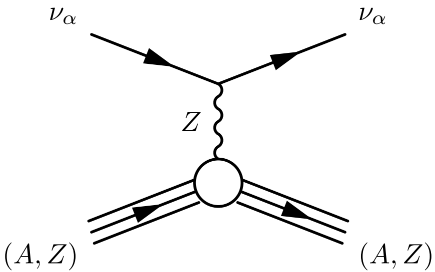

coherency limit: $|\vec{q}| \leq 1/R_{\text{nucleus}}$

- 3-momentum transfer $|\vec{q}| = \sqrt{2MT} = \sqrt{2E_\nu^2(1-\cos\theta)}$
- M: nuclear mass
- E_ν: incident neutrino energy
- T: nuclear recoil energy
- θ: scattering angle

CEνNS has a really large cross section, but...

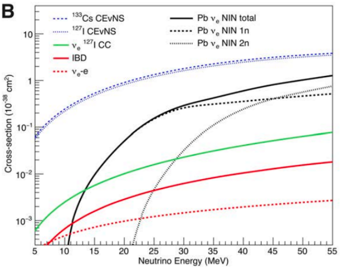

characteristic N^2 dependence

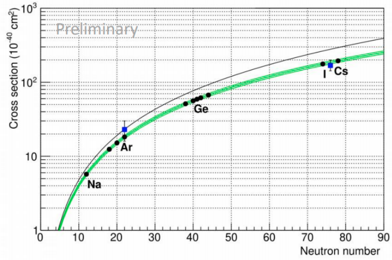

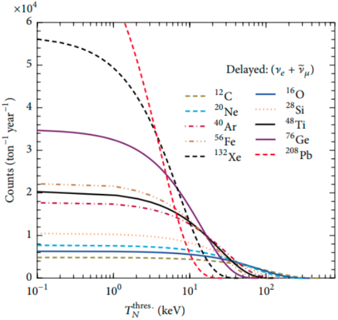

push-pull:

heavy nucleus $\rightarrow \sigma_{\text{CEvNS}} \rightarrow T_{\text{max}}$

$$T_{\text{max}} = \frac{2E_\nu^2}{M} \sim \text{keV}$$

Physics Motivations of CEνNS

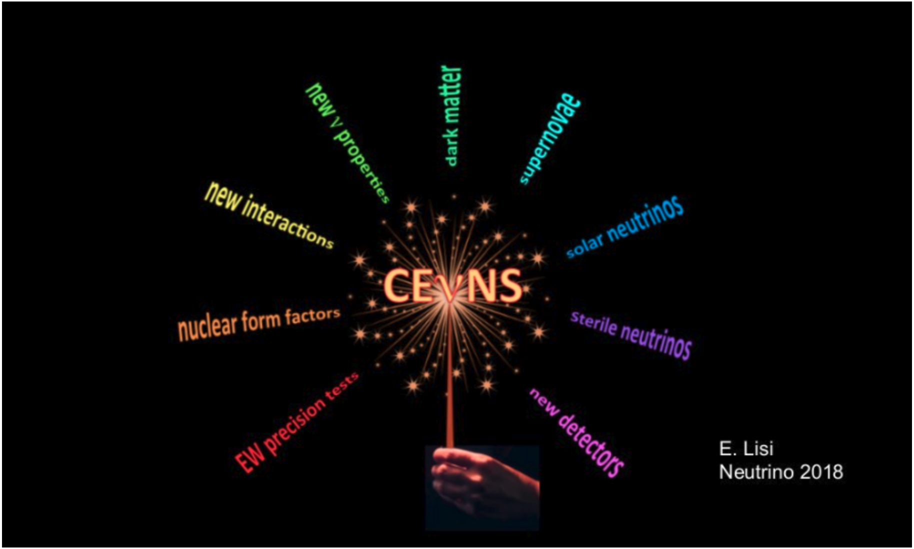

CEνNS experiments worldwide

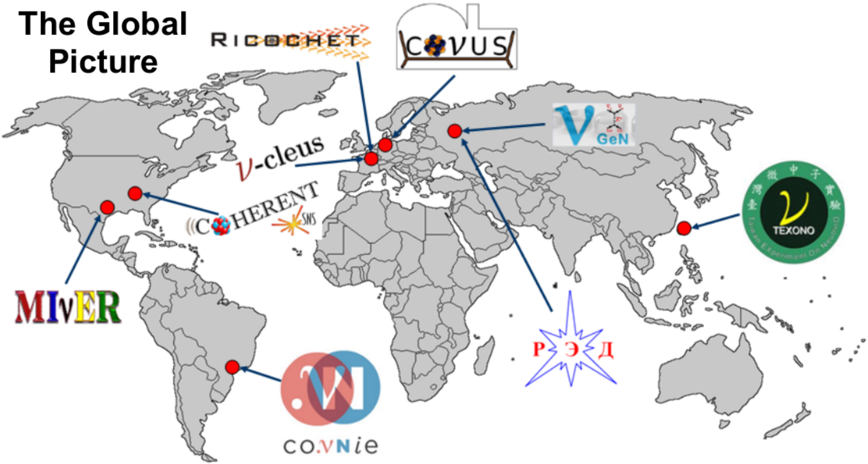

from M. Green: Aspen 2019 Winter Conference, March 2019

+ SBC (Mexico), vIOLETA (Argentina), ESS (Sweden), CCM (USA)

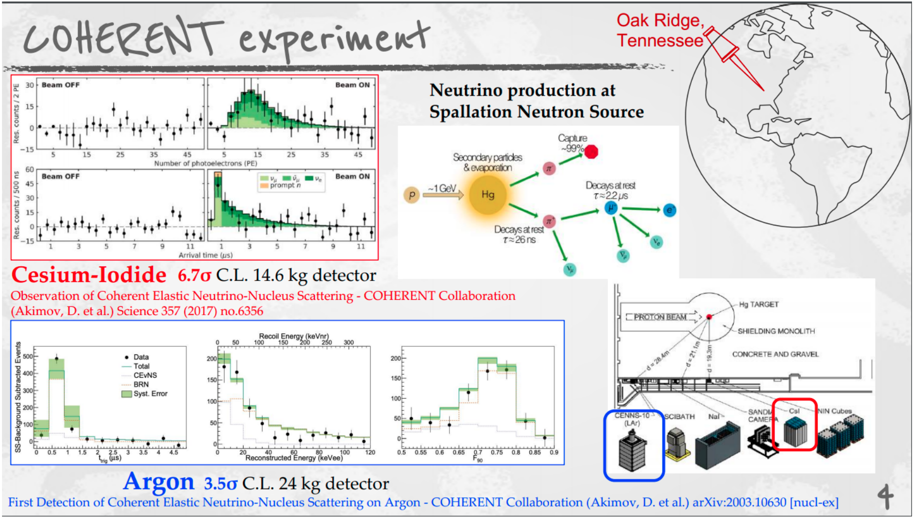

from N. Cargioli: Magnificent CEvNS 2020

Standard Model physics & nuclear structure

Standard Model CEνNS cross section

CEνNS cross section expressed through the nuclear recoil energy T_A

$$\left(\frac{d\sigma}{dT_A}\right)_{\text{SM}} = \frac{G_F^2 m_A}{\pi}\left[\mathcal{Q}_V^2\left(1-\frac{m_A T_A}{2E_\nu^2}\right)+\mathcal{Q}_A^2\left(1+\frac{m_A T_A}{2E_\nu^2}\right)\right]F^2(Q^2)$$

[DKP, Kosmas: PRD 97 (2018)]

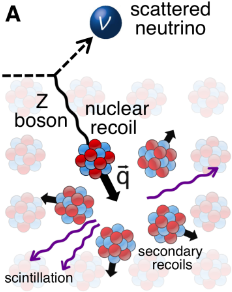

- E_ν: is the incident neutrino energy
- m_A: the nuclear mass of the detector material
- Z protons and $N = A - Z$ neutrons
- vector $\mathcal{Q}_V$ and axial vector $\mathcal{Q}_A$ contributions
- $F(Q^2)$: is the nuclear form factor

$$\mathcal{Q}_V = \left[2(g_u^L+g_u^R)+(g_d^L+g_d^R)\right]Z+\left[(g_u^L+g_u^R)+2(g_d^L+g_d^R)\right]N\,,$$

$$\mathcal{Q}_A = \left[2(g_u^L-g_u^R)+(g_d^L-g_d^R)\right](\delta Z)+\left[(g_u^L-g_u^R)+2(g_d^L-g_d^R)\right](\delta N)\,,$$

- $(\delta Z) = Z_+ - Z_-$ and $(\delta N) = N_+ - N_-$, where Z_+ (N_+) and Z_- (N_-) refers to total number of protons (neutrons) with spin up or down [Barranco et al.: JHEP 0512 (2005)]

Standard Model CEνNS cross section

CEνNS cross section expressed through the nuclear recoil energy T_A

$$\left(\frac{d\sigma}{dT_A}\right)_{\rm SM} = \frac{G_F^2 m_A}{\pi}\left[\mathcal{Q}_V^2\left(1-\frac{m_A T_A}{2E_\nu^2}\right)+\mathcal{Q}_A^2\left(1+\frac{m_A T_A}{2E_\nu^2}\right)\right] F^2(Q^2)$$

[DKP, Kosmas: PRD 97 (2018)]

- E_ν: is the incident neutrino energy
- m_A: the nuclear mass of the detector material
- Z protons and $N = A - Z$ neutrons
- vector $\mathcal{Q}_V$ and axial vector $\mathcal{Q}_A$ contributions
- $F(Q^2)$: **is the nuclear form factor**

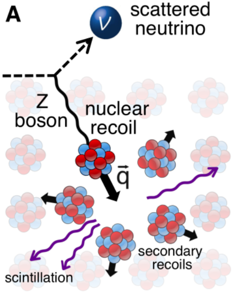

$$\mathcal{Q}_V = \left[\frac{1}{2} - 2\sin^2\theta_W\right] Z - \frac{1}{2} N\,,$$

$$\mathcal{Q}_A = \frac{1}{2}(\delta Z) + \frac{1}{2}(\delta N)\,,$$

- weak mixing angle: $\sin^2\theta_W$ not well measured at low energies

Nuclear rms radius

The CEnNS process as unique probe of the neutron density distribution of nuclei

The CEnNS process itself can be used to provide the first **model independent measurement of the neutron distribution radius**, which is basically unknown for most of the nuclei.

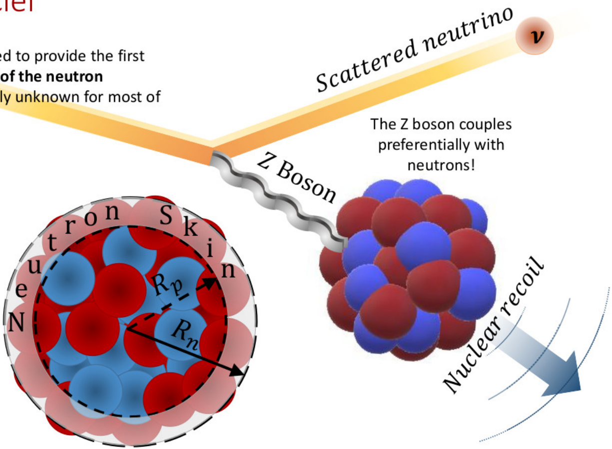

Even if it sounds strange, spatial distribution of neutrons inside nuclei is basically unknown!

The rms neutron distribution radius Rn and the difference between Rn and the rms radius Rp of the proton distribution (the so-called "**neutron skin**")

slide from: M. Cadeddu @ NuFact 2018

Evaluation of the form factors (Klein-Nystrand)

Papoulias et al. PLB 800 (2020) 135133

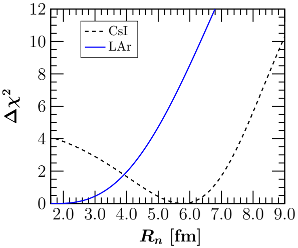

Follows from the convolution of a Yukawa potential with range $a_k = 0.7$ fm over a Woods-Saxon distribution, approximated as a hard sphere with radius R_A.

$$F_{\rm KN} = 3\frac{j_1(QR_A)}{qR_A}\left[1+(Qa_k)^2\right]^{-1}$$

The rms radius is: $\langle R^2\rangle_{\rm KN} = 3/5R_A^2 + 6a_k^2$

Klein, Nystrand, PRC 60 (1999) 014903

Cadeddu et al., arXiv:2102.06153

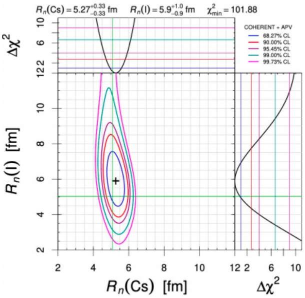

First data driven determination of the neutron rms radius

Evaluation of the form factors (Helm)

Convolution of two nucleonic densities, one being a uniform density with cut-off radius R_0, (namely box or diffraction radius) characterizing the interior density and a second one that is associated with a Gaussian falloff in terms of the surface thickness s.

$$F_{\text{Helm}}(Q^2) = F_B F_G = 3\frac{j_1(QR_0)}{qR_0}\, e^{-(Qs)^2/2}$$

The first three moments

$$\langle R_n^2 \rangle = \frac{3}{5} R_0^2 + 3s^2$$
$$\langle R_n^4 \rangle = \frac{3}{7} R_0^4 + 6R_0^2 s^2 + 15 s^4$$
$$\langle R_n^6 \rangle = \frac{1}{3} R_0^6 + 9R_0^4 s^2 + 63 R_0^2 s^4 + 105 s^6\,.$$

- $j_1(x)$ is the known first-order Spherical-Bessel function
- box or diffraction radius R_0 (interior density)
- $s = 0.9$ fm: surface thickness of the nucleus from spectroscopy data (Gaussian fallof).

J. Engel, Phys.Lett. **B 264** (1991) 114

Evaluation of the form factors (Symmetrized Fermi)

Adopting a conventional Fermi (Woods-Saxon) charge density distribution, the SF form factor is written in terms of two parameters (c, a)

$$F_{\mathrm{SF}}\left(Q^2\right) = \frac{3}{Qc\left[(Qc)^2 + (\pi Q a)^2\right]}\left[\frac{\pi Q a}{\sinh(\pi Q a)}\right]\left[\frac{\pi Q a \sin(Qc)}{\tanh(\pi Q a)} - Qc\cos(Qc)\right],$$

The first three moments

$$\begin{aligned}
\left\langle R_n^2\right\rangle &= \frac{3}{5}c^2 + \frac{7}{5}(\pi a)^2 \\
\left\langle R_n^4\right\rangle &= \frac{3}{7}c^4 + \frac{18}{7}(\pi a)^2 c^2 + \frac{31}{7}(\pi a)^4 \\
\left\langle R_n^6\right\rangle &= \frac{1}{3}c^6 + \frac{11}{3}(\pi a)^2 c^4 + \frac{239}{15}(\pi a)^4 c^2 + \frac{127}{5}(\pi a)^6 .
\end{aligned}$$

- c: half-density radius
- a fm: diffuseness
- surface thickness: $t = 4a\ln 3$

J.D. Lewin and P.F. Smith, Astropart.Phys. 6 (1996) 87-112

Nuclear structure models: BCS calculations

Within the context of the quasi-particle random phase approximation (QRPA) method the form factors for protons (neutrons) are obtained as

$$F_{N_n} = \frac{1}{N_n} \sum_j \hat{j} \langle g.s. || j_0(|\mathbf{q}|r) || g.s. \rangle \left(v_j^{p(n)} \right)^2$$

where $\hat{j} = \sqrt{2j+1}$, $N_n = Z$ (or N), $v_j^{p(n)}$ are the BCS probability amplitudes, determined by solving iteratively the BCS equations.

T.S. Kosmas, J.D. Vergados, O. Civitarese and A. Faessler, NPA 570 (1994) 637

After choosing the active model space the following important parameters must be properly adjusted

- the harmonic oscillator (h.o.) size parameter b
- the two pairing parameters $g_{\rm pair}^{p\,(n)}$ for proton (neutron) pairs that renormalise the monopole (pairing) residual interaction of the Bonn C-D two-body potential (describing the strong two-nucleon forces)

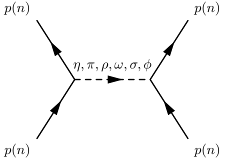

- *Realistic proton and neutron form factors*
- The Bonn C-D residual interaction is mediated via one-meson exchange

  R. Machleidt, Phys.Rev. **C63** (2001) 024001

Nuclear structure models: deformed shell model

Kota & Sahu: *Structure of Medium Mass Nuclei: Deformed Shell Model and Spin-Isospin Interacting Boson Model*, CRC Press

- **Assume axial symmetry**
- **Model space**: a set single-particle (sp) orbitals + an effective two-body Hamiltonian
- **Lowest-energy intrinsic states**: by solving the HF single-particle equation self-consistently.
- **Excited intrinsic configurations**: via particle-hole excitations over the lowest intrinsic state.
- **Problem!** Intrinsic states $\chi_K(\eta)$: do not have definite angular momenta

States of good angular momentum, projected from an intrinsic state $\chi_K(\eta)$

$$|\psi^J_{MK}(\eta)\rangle = \frac{2J+1}{8\pi^2\sqrt{N_{JK}}}\int d\Omega D^{J^*}_{MK}(\Omega)R(\Omega)|\chi_K(\eta)\rangle \,,$$

where N_{JK} is the normalization constant given by

$$N_{JK} = \frac{2J+1}{2}\int_0^\pi d\beta \sin\beta d^J_{KK}(\beta)\langle\chi_K(\eta)|e^{-i\beta J_y}|\chi_K(\eta)\rangle \,.$$

- $R(\Omega) = \exp(-i\alpha J_z)\exp(-i\beta J_y)\exp(-i\gamma J_z)$: general rotation operator
- Ω: the Euler angles (α, β, γ)
- $|\psi^J_{MK}(\alpha)\rangle$ projected from different intrinsic states are not in general orthogonal to each other

Band mixing calculations are performed after appropriate orthonormalization. The resulting eigenfunctions are of the form

$$|\Phi^J_M(\eta)\rangle = \sum_{K,\alpha} S^J_{K\eta}(\alpha)|\psi^J_{MK}(\alpha)\rangle \,, \qquad S^J_{K\eta}(\alpha): \text{ expansion coefficients}$$

The nuclear matrix elements occurring in the calculation of magnetic moments, elastic and inelastic spin structure functions etc. are evaluated using the wave functions $|\Phi^J_M(\eta)\rangle$.

Comparison of the nuclear methods

DKP, Kosmas, Adv.High Energy Phys. **2015** (2015) 763648

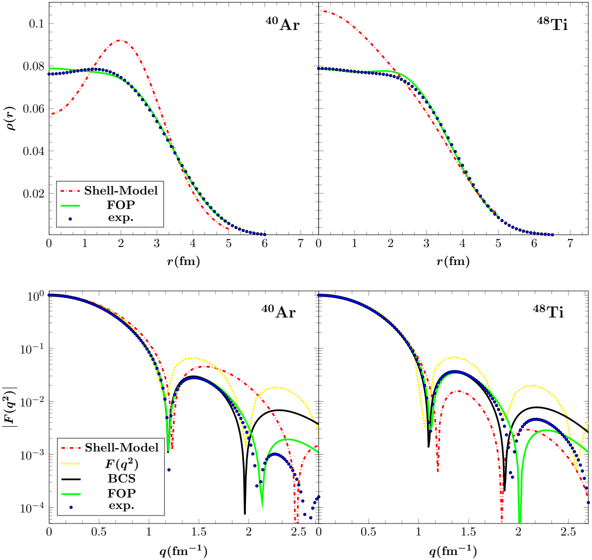

Probing nuclear form factors: COHERENT exp.

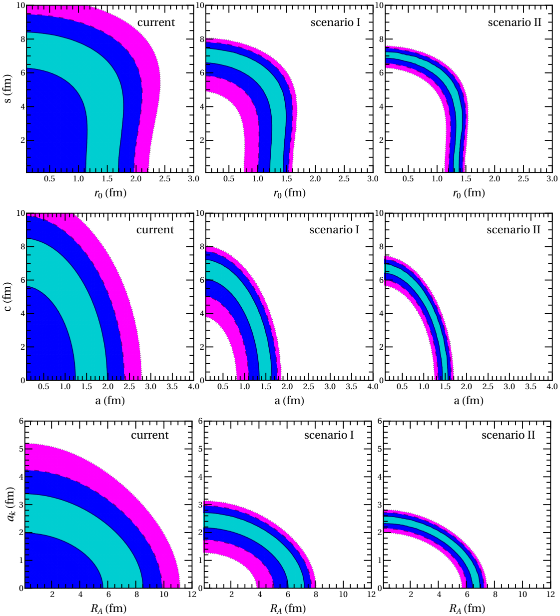

DKP, Kosmas, Sahu, Kota, Hota PLB 800 (2020) 135133

Impact of form factor on CEνNS: COHERENT exp.

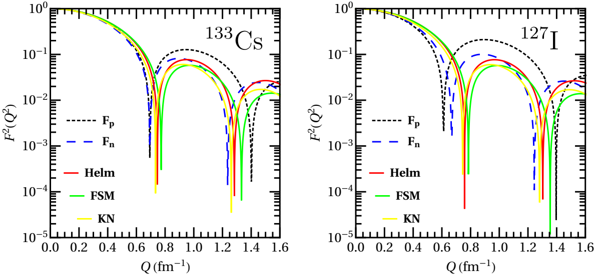

DKP, Kosmas, Sahu, Kota, Hota PLB 800 (2020) 135133

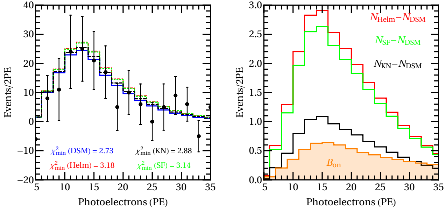

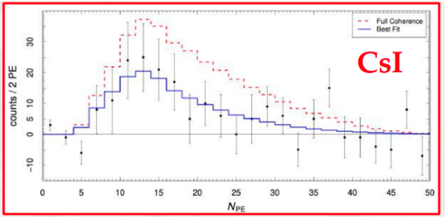

M. Cadeddu et al. - Phys.Rev.D 101 (2020) 3, 033004

Standard Model precision tests (away from the Z-pole)

current situation from COHERENT

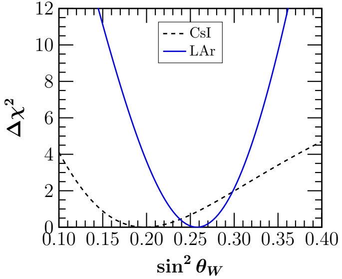

Miranda et al. JHEP 05 (2020) 130

future measurements can do better

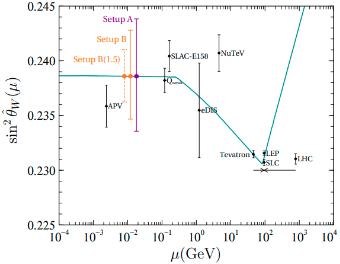

[SBC Collaboration] L. J. Flores et al.

JPhys.Rev.D 103 (2021) 9, L091301

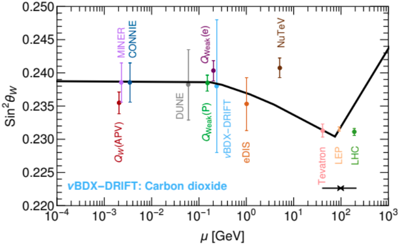

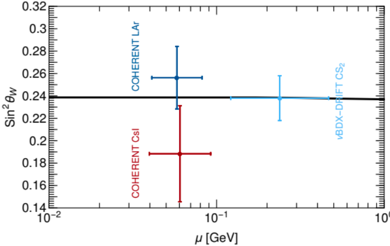

Aristizabal et al. arXiv: 2103.10857

Incoherent neutrino-nucleus scattering

Naumov Bednyakov formalism

$$\frac{d\sigma_{\rm inc}}{dT_A} = \frac{4G_F^2 m_A}{\pi} \sum_{f=n,p} g_{\rm inc}^f \left(1 - |F_f|^2\right) \times \left[A_+^f \left(\left(g_{L,f} - g_{R,f}\, ab^2\right)^2 + g_{R,f}^2\, ab^2 (1-a) \right) + A_-^f g_{R,f}^2 (1-a)\left(1 - a + ab^2\right) \right]. \tag{1}$$

$$a = \frac{q^2}{q_{\rm min}^2} \simeq \frac{T_A}{T_A^{\rm max}}, \quad b^2 = \frac{m_f^2}{s}\,. \tag{2}$$

Here, $A_\pm^p \equiv Z_\pm$ ($A_\pm^n \equiv N_\pm$) represents the number of protons (neutrons) with spin $\pm 1/2$ and $s = (p+k)^2$ is the total energy squared in the center-of-mass frame (p denotes an effective 4-momentum of the nucleon).

Bednyakov, Naumov, PRD 98 (2018) 053004

For a more detailed study see: [Hoferichter, Menéndez, Schwenk PRD 102, 074018

Incoherent vs. Coherent rates: πDAR and reactors

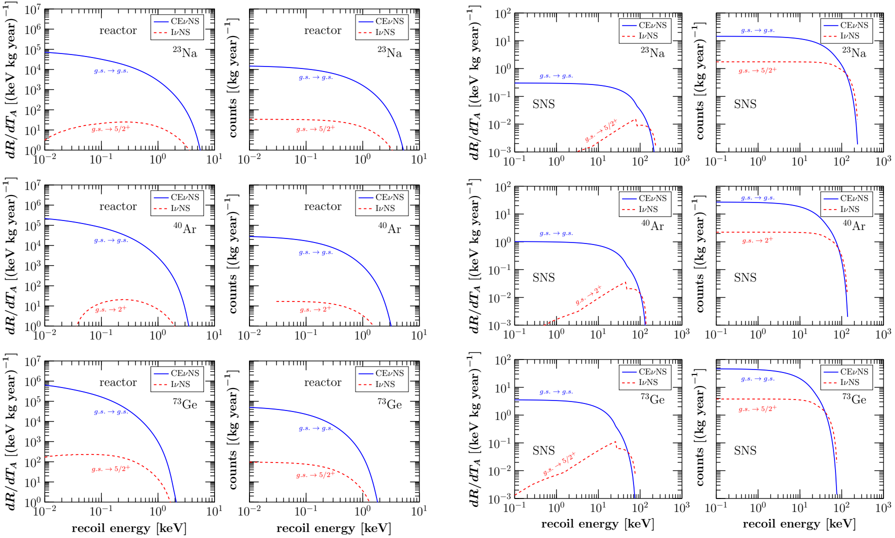

Sahu, DKP, Kota, Kosmas, PRC 102 (2020) 3, 035501

Non Standard Interactions (NSIs)

NSI Phenomenological description

Similarly, the Lagrangian describing non-standard neutrino interactions (NSI), reads

$$\mathcal{L}_{\rm NSI} = -2\sqrt{2}G_F \sum_{\substack{f=u,d \\ \alpha,\beta=e,\mu,\tau}} \epsilon_{\alpha\beta}^{fP} \left[\bar{\nu}_\alpha \gamma_\rho L \nu_\beta\right] \left[\bar{f}\gamma^\rho P f\right]$$

J. Barranco, O.G. Miranda, C.A. Moura and J.W.F. Valle, PRD 73 (2006) 113001

O.G. Miranda, M.A. Tortola and J.W.F. Valle, JHEP 0610 (2006) 008

- *flavour preserving non-universal (NU) terms* proportional to $\epsilon_{\alpha\alpha}^{fP}$.
- *flavour-changing (FC) terms* proportional to $\epsilon_{\alpha\beta}^{fP}$, $\alpha \neq \beta$.

The couplings with respect to the Fermi coupling constant G_F

are of vector and axial vector type, as

- vector couplings: $\epsilon_{\alpha\beta}^{fV} = \epsilon_{\alpha\beta}^{fL} + \epsilon_{\alpha\beta}^{fR}$
- axial-vector couplings: $\epsilon_{\alpha\beta}^{fA} = \epsilon_{\alpha\beta}^{fL} - \epsilon_{\alpha\beta}^{fR}$

S. Davidson et. al., JHEP 03 (2003) 011
J. Barranco, O.G. Miranda and T.I. Rashba, JHEP 0512 (2005) 021

K. Scholberg, PRD 73 (2006) 033005

NSI Cross sections and Nuclear Transition Matrix Elements

NSI CEνNS diff. cross section with respect to the scattering angle θ

$$\frac{d\sigma_{\mathrm{NSI},\nu_\alpha}}{d\cos\theta} = \frac{G_F^2}{2\pi} E_\nu^2 (1+\cos\theta) \left| \langle g.s.|| G_{V,\nu_\alpha}^{\mathrm{NSI}}(Q) || g.s. \rangle \right|^2, \ (\alpha = e, \mu, \tau)$$

DKP and T.S. Kosmas, Phys.Lett. **B728** (2014) 482

- The corresponding NSI nuclear matrix element (ME) are now written as

$$\left| \mathcal{M}_{V,\nu_\alpha}^{\mathrm{NSI}} \right|^2 \equiv \left| \langle g.s.|| G_{V,\nu_\alpha}^{\mathrm{NSI}}(Q) || g.s. \rangle \right|^2 =$$
$$\left[\left(g_V^p + 2\epsilon_{\alpha\alpha}^{uV} + \epsilon_{\alpha\alpha}^{dV} \right) Z F_Z(Q^2) + \left(g_V^n + \epsilon_{\alpha\alpha}^{uV} + 2\epsilon_{\alpha\alpha}^{dV} \right) N F_N(Q^2) \right]^2$$
$$+ \sum_{\beta \neq \alpha} \left[\left(2\epsilon_{\alpha\beta}^{uV} + \epsilon_{\alpha\beta}^{dV} \right) Z F_Z(Q^2) + \left(\epsilon_{\alpha\beta}^{uV} + 2\epsilon_{\alpha\beta}^{dV} \right) N F_N(Q^2) \right]^2$$

- The flavour preserving (FP) ME (obtained from $\mathcal{L}_{\mathrm{FP}} \equiv \mathcal{L}_{\mathrm{SM}} + \mathcal{L}_{\mathrm{NU}}$)

$$\left| \mathcal{M}_{V,\nu_\alpha}^{\mathrm{FP}} \right|^2 = \left| \mathcal{M}_{V,\nu_\alpha}^{\mathrm{SM}} + \mathcal{M}_{V,\nu_\alpha}^{\mathrm{NU}} \right|^2 .$$

- The total coherent cross section is computed on the basis of the ME

$$\left| \mathcal{M}_{V,\nu_\alpha}^{\mathrm{NSI}} \right|^2 \equiv \left| \mathcal{M}_{V,\nu_\alpha}^{\mathrm{tot}} \right|^2 = \left| \mathcal{M}_{V,\nu_\alpha}^{\mathrm{FP}} \right|^2 + \left| \mathcal{M}_{V,\nu_\alpha}^{\mathrm{FC}} \right|^2 .$$

DKP and T.S. Kosmas, Adv.High Energy Phys. **2015** (2015) 763648

NSI Analysis of COHERENT-CsI data

DKP and T.S. Kosmas, Phys.Rev. **D97** (2018) 033003

see also Giunti PRD 101, 035039 (2020)

- **vector NSI:** $\mathcal{O}^{qV}_{\alpha\beta} = (\bar{\nu}_\alpha \gamma^\mu L \nu_\beta)\,(\bar{q}\gamma_\mu P q)$
  CEνNS cross section becomes flavor dependent through the substitution $\mathcal{Q}^V_W \to \mathcal{Q}^V_{\rm NSI}$
- **NSI vector couplings**

$$\mathcal{Q}^V_{\rm NSI} = (2\epsilon^{uV}_{\alpha\alpha} + \epsilon^{dV}_{\alpha\alpha} + g^V_p)Z + (\epsilon^{uV}_{\alpha\alpha} + 2\epsilon^{dV}_{\alpha\alpha} + g^V_n)N + \sum_{\alpha,\beta}\left[(2\epsilon^{uV}_{\alpha\beta} + \epsilon^{dV}_{\alpha\beta})Z + (\epsilon^{uV}_{\alpha\beta} + 2\epsilon^{dV}_{\alpha\beta})N\right] .$$

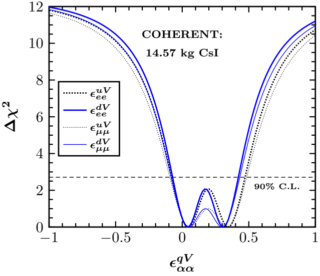

impact of nuclear uncertainties

- **Neutrino Generalized Interactions (NGI)**

$$\mathscr{L}_S \sim (\bar{\nu}\nu)\left[\bar{q}\left(C^q_S + i\gamma_5 D^q_S\right)q\right]$$
$$\mathscr{L}_P \sim (\bar{\nu}\gamma_5\nu)\left[\bar{q}\left(\gamma_5 C^q_P + i D^q_P\right)q\right]$$
$$\mathscr{L}_V \sim (\bar{\nu}\gamma^\mu\nu)\left[\bar{q}\left(\gamma_\mu C^q_V + i\gamma_\mu\gamma_5 D^q_V\right)q\right]$$
$$\mathscr{L}_A \sim (\bar{\nu}\gamma^\mu\gamma_5\nu)\left[\bar{q}\left(\gamma_\mu\gamma_5 C^q_A + i\gamma_\mu D^q_A\right)q\right]$$
$$\mathscr{L}_T \sim (\bar{\nu}\sigma^{\mu\nu}\nu)\left[\bar{q}\left(\sigma_{\mu\nu} C^q_T + i\sigma_{\mu\nu}\gamma_5 D^q_T\right)q\right]$$

Aristizabal, De Romeri, Rojas, PRD98 (2018) 075018

Aristizabal, Liao, Marfatia, JHEP 1906 141 (2019)

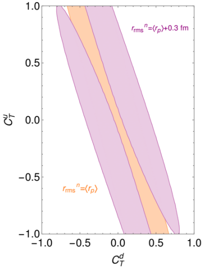

COHERENT-CsI vs. COHERENT-LAr data

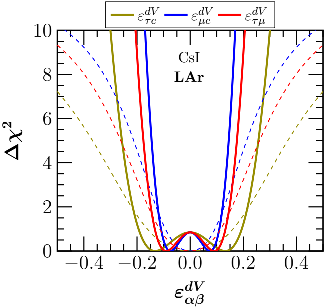

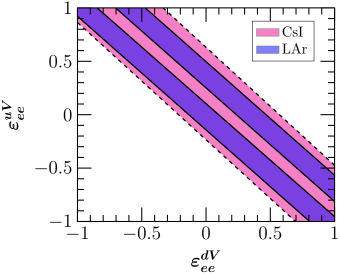

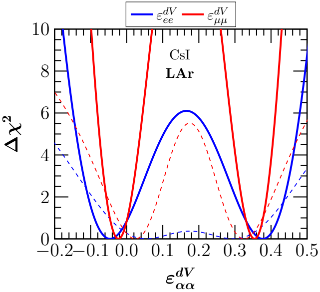

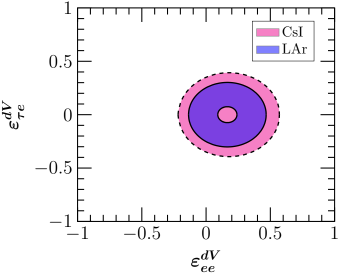

Miranda et al. JHEP 05 (2020) 130

NSIs from string-inspired E_6 theories

$$\varepsilon_u^L = -4\gamma \hat{s}_Z^2 \rho_{\nu N}^{NC} \left(\frac{c_\beta}{\sqrt{24}} - \frac{s_\beta}{3}\sqrt{\frac{5}{8}}\right)\left(\frac{3c_\beta}{2\sqrt{24}} + \frac{s_\beta}{6}\sqrt{\frac{5}{8}}\right),$$

$$\varepsilon_d^R = -8\gamma \hat{s}_Z^2 \rho_{\nu N}^{NC} \left(\frac{3c_\beta}{2\sqrt{24}} + \frac{s_\beta}{6}\sqrt{\frac{5}{8}}\right)^2,$$

$$\varepsilon_d^L = \varepsilon_u^L = -\varepsilon_u^R,$$

with $c_\beta = \cos\beta$, $s_\beta = \sin\beta$, $\gamma = (M_Z/M_{Z'})^2$.
E_6 models: (χ, ψ, η) corresponding to $\cos\beta = (1, 0, \sqrt{3/8})$.

	T_3	$\sqrt{40}Y_\chi$	$\sqrt{24}Y_\psi$
Q	$\begin{pmatrix}1/2\\-1/2\end{pmatrix}$	-1	1
u^c	0	-1	1
e^c	0	-1	1
d^c	0	3	1
l	$\begin{pmatrix}1/2\\-1/2\end{pmatrix}$	3	1

Barranco, Miranda, Rashba, PRD 76, 073008

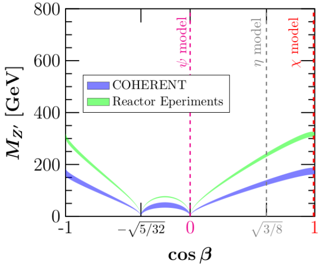

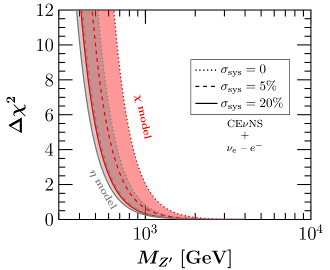

Miranda et al. PRD 101 (2020) 7, 073005

Light vector and scalar mediators

- **vector Z' mediator** Dutta et al. PRD 93 (2016) 013015
  $\mathcal{L}_{\rm vec} = Z'_\mu \left(g^{qV}_{Z'} \bar{q}\gamma^\mu q + g^{\nu V}_{Z'} \bar{\nu}_L \gamma^\mu \nu_L \right) + \frac{1}{2} M^2_{Z'} Z'_\mu Z'^\mu$
- **Z' contribution to CEνNS cross section**

$$\left(\frac{d\sigma}{dT_N} \right)_{\rm SM+Z'} = \mathcal{G}^2_{Z'}(T_N) \frac{d\sigma_{\rm SM}}{dT_N} ,$$

$$\mathcal{G}_{Z'} = 1 + \frac{1}{\sqrt{2} G_F} \frac{\mathcal{Q}_{Z'}}{\mathcal{Q}_W^V} \frac{g^{\nu V}_{Z'}}{2MT_N + M^2_{Z'}} ,$$

- **Z' charge:** $\mathcal{Q}_{Z'} = \left(2g^{uV}_{Z'} + g^{dV}_{Z'} \right) Z + \left(g^{uV}_{Z'} + 2g^{dV}_{Z'} \right) N$

- **Scalar ϕ mediator** Dent et al. PRD 96 (2017) 095007
  $\mathcal{L}_{\rm sc} = \phi \left(g^{qS}_\phi \bar{q}q + g^{\nu S}_\phi \bar{\nu}_R \nu_L + {\rm H.c.} \right) - \frac{1}{2} M^2_\phi \phi^2$
- **ϕ contribution to CEνNS cross section**

$$\left(\frac{d\sigma}{dT_N} \right)_{\rm scalar} = \frac{G_F^2 M^2}{4\pi} \frac{\mathcal{G}^2_\phi M^4_\phi T_N}{E^2_\nu \left(2MT_N + M^2_\phi \right)^2} F^2(T_N)$$

$$\mathcal{G}_\phi = \frac{g^{\nu S}_\phi \mathcal{Q}_\phi}{G_F M^2_\phi}$$

- **scalar charge:** $\mathcal{Q}_\phi = \sum_{\mathcal{N},q} g^{qS}_\phi \frac{m_\mathcal{N}}{m_q} f^{(\mathcal{N})}_{T,q}$

see also Flores, Nath, Peinado JHEP 06 (2020) 045

M. Cadeddu et al. JHEP 01 (2021) 116

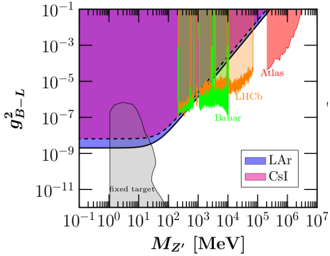

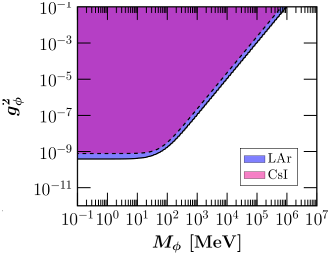

Miranda et al. JHEP 05 (2020) 130

Impact of the quenching factor

Konovalov, Magnificent CEvNS 2020

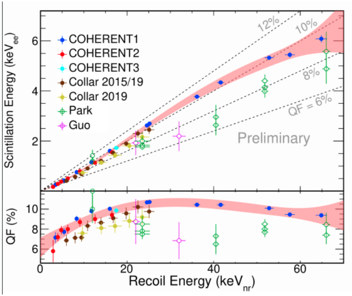

Papoulias PRD 102 (2020) 11, 113004

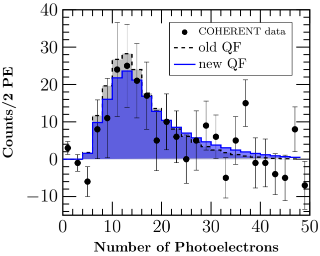

sensitivities improved

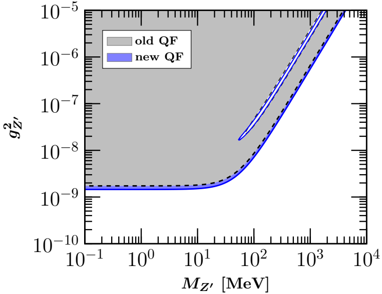

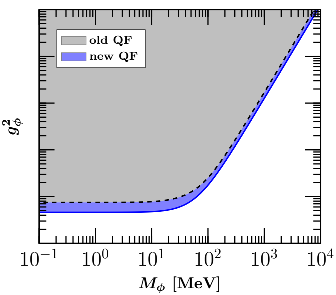

Electromagnetic neutrino properties

Electromagnetic contribution to CEνNS cross section

The Electromagnetic CEνNS cross section reads [Vogel, Engel.: PRD 39 [1989] 3378

$$\left(\frac{d\sigma}{dT_A}\right)_{\mathrm{EM}} = \frac{\pi a_{\mathrm{EM}}^2 \mu_\nu^2 Z^2}{m_e^2} \left(\frac{1 - T_A/E_\nu}{T_A}\right) F^2(Q^2) \, .$$

- can be dominant for sub-keV threshold experiments
- may lead to detectable distortions of the recoil spectrum

The helicity preserving SM cross section adds incoherently with the helicity-violating EM cross section

$$\left(\frac{d\sigma}{dT_A}\right)_{\mathrm{tot}} = \left(\frac{d\sigma}{dT_A}\right)_{\mathrm{SM}} + \left(\frac{d\sigma}{dT_A}\right)_{\mathrm{EM}}$$

μ_ν^2 is the effective neutrino magnetic moment in the mass basis relevant to a given neutrino beam (reactor, SNS, etc.)

- Experimental measurements usually constrain some process-dependent effective parameter combination
- needs to be expressed in terms of fundamental parameters (TMMs + CP phases + mixing-angles)
- Even in the case of laboratory neutrino experiments, where the initial neutrino flux is fixed to have a well determined given flavor, there is no sensitivity to the final neutrino state

Electromagnetic neutrino vertex (spin component)

Dirac neutrinos: $H^{\mathrm{D}}_{\mathsf{EM}} = \frac{1}{2}\bar{\nu}_R \lambda \sigma^{\alpha\beta} \nu_L F_{\alpha\beta} + \mathrm{h.c.}$

- $\lambda = \mu - i\epsilon$ is an arbitrary complex matrix
- $\mu = \mu^\dagger$ and $\epsilon = \epsilon^\dagger$.

Majorana neutrinos: $H^{\mathrm{M}}_{\mathsf{EM}} = -\frac{1}{4}\nu_L^{\mathsf{T}} C^{-1} \lambda \sigma^{\alpha\beta} \nu_L F_{\alpha\beta} + \mathrm{h.c.}$

- $\lambda = \mu - i\epsilon$: antisymmetric complex matrix ($\lambda_{\alpha\beta} = -\lambda_{\beta\alpha}$)
- $\mu^{\mathsf{T}} = -\mu$ and $\epsilon^{\mathsf{T}} = -\epsilon$ are two imaginary matrices.
- three complex or six real parameters are required

In contrast to the Dirac case, vanishing diagonal moments are implied for Majorana neutrinos, $\mu^{\mathrm{M}}_{ii} = \epsilon^{\mathrm{M}}_{ii} = 0$.

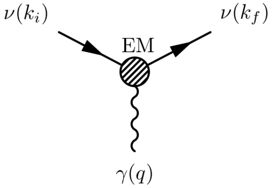

[Schechter, Valle: PRD 24 (1981), PRD 25 (1982)]

The neutrino transition magnetic moment (TMM) matrix

The magnetic moment matrix λ ($\tilde{\lambda}$) in the flavor (mass) basis reads

[Tórtola: PoS AHEP 2003 (2003)]

$$\lambda = \begin{pmatrix} 0 & \Lambda_\tau & -\Lambda_\mu \\ -\Lambda_\tau & 0 & \Lambda_e \\ \Lambda_\mu & -\Lambda_e & 0 \end{pmatrix}, \qquad \tilde{\lambda} = \begin{pmatrix} 0 & \Lambda_3 & -\Lambda_2 \\ -\Lambda_3 & 0 & \Lambda_1 \\ \Lambda_2 & -\Lambda_1 & 0 \end{pmatrix}$$

- the definition $\lambda_{\alpha\beta} = \varepsilon_{\alpha\beta\gamma}\Lambda_\gamma$ has been introduced,
- the neutrino TMMs are represented by the complex parameters

$$\Lambda_\alpha = |\Lambda_\alpha| e^{i\zeta_\alpha}, \qquad \Lambda_i = |\Lambda_i| e^{i\zeta_i}$$

three complex or six real parameters (3 moduli + 3 phases)

Effective neutrino magnetic moment @ experiments

Is expressed in terms of the neutrino magnetic moment matrix and the amplitudes of positive and negative helicity states 3−vectors $\mathfrak{a}_+$ and $\mathfrak{a}_-$,

- In the flavor basis one finds [Grimus, Schwetz: Nucl. Phys. B587 (2000)]

$$\left(\mu_\nu^F\right)^2 = \mathfrak{a}_-^\dagger \lambda^\dagger \lambda \mathfrak{a}_- + \mathfrak{a}_+^\dagger \lambda \lambda^\dagger \mathfrak{a}_+ \,,$$

Introducing the transformations (U is the lepton mixing matrix)

$$\tilde{\mathfrak{a}}_- = U^\dagger \mathfrak{a}_-, \qquad \tilde{\mathfrak{a}}_+ = U^\mathsf{T} \mathfrak{a}_+, \qquad \tilde{\lambda} = U^\mathsf{T} \lambda U \,,$$

- In the mass basis reads

$$\left(\mu_\nu^M\right)^2 = \tilde{\mathfrak{a}}_-^\dagger \tilde{\lambda}^\dagger \tilde{\lambda} \tilde{\mathfrak{a}}_- + \tilde{\mathfrak{a}}_+^\dagger \tilde{\lambda} \tilde{\lambda}^\dagger \tilde{\mathfrak{a}}_+$$

TMMs in flavor & mass basis @ reactor facilities

Reactor antineutrinos: $\bar{\nu}_e$ (with $\mathfrak{a}_+^1 = 1$)

- flavor basis

$$\left(\mu^F_{\bar{\nu}_e,\,\text{reactor}}\right)^2 = |\Lambda_\mu|^2 + |\Lambda_\tau|^2$$

where $|\Lambda_\mu|$ and $|\Lambda_\tau|$ are the elements of the neutrino TMM matrix λ describing the corresponding conversions from the electron antineutrino to the muon and tau neutrino states

- mass basis [Cañas et al.: PLB 753 (2016)]

$$\begin{aligned}\left(\mu^M_{\bar{\nu}_e,\,\text{reactor}}\right)^2 =& |\boldsymbol{\Lambda}|^2 - c_{12}^2 c_{13}^2 |\Lambda_1|^2 - s_{12}^2 c_{13}^2 |\Lambda_2|^2 - s_{13}^2 |\Lambda_3|^2 \\ & - c_{13}^2 \sin 2\theta_{12} |\Lambda_1||\Lambda_2| \cos\xi_3 \\ & - c_{12} \sin 2\theta_{13} |\Lambda_1||\Lambda_3| \cos(\delta_{\text{CP}} - \xi_2) \\ & - s_{12} \sin 2\theta_{13} |\Lambda_2||\Lambda_3| \cos(\delta_{\text{CP}} - \xi_1)\,,\end{aligned}$$

with $|\boldsymbol{\Lambda}|^2 = |\Lambda_1|^2 + |\Lambda_2|^2 + |\Lambda_3|^2$ and

phase redefinition: $\xi_1 = \zeta_3 - \zeta_2$, $\xi_2 = \zeta_3 - \zeta_1$ and $\xi_3 = \zeta_1 - \zeta_2$

TMMs in flavor & mass basis @ SNS facilities (prompt)

Prompt beam: ν_μ (with $\mathfrak{a}_-^2 = 1$)

- flavor basis

$$\left(\mu^F_{\nu_\mu,\,\text{prompt}}\right)^2 = |\Lambda_e|^2 + |\Lambda_\tau|^2$$

- mass basis

$$\begin{aligned}
\left(\mu^M_{\nu_\mu,\,\text{prompt}}\right)^2 = & |\Lambda_1|^2 \left[-2c_{12}c_{23}s_{12}s_{13}s_{23}\cos\delta_{\text{CP}} + s_{23}^2\left(c_{13}^2 + s_{12}^2 s_{13}^2\right) + c_{12}^2 c_{23}^2\right] \\
& + |\Lambda_2|^2 \left[2c_{12}c_{23}s_{13}s_{23}s_{12}\cos\delta_{\text{CP}} + c_{23}^2 s_{12}^2 + s_{23}^2\left(c_{12}^2 s_{13}^2 + c_{13}^2\right)\right] \\
& + |\Lambda_3|^2 \left[c_{23}^2 + s_{13}^2 s_{23}^2\right] \\
& + 2\,|\Lambda_1\Lambda_2| \left[c_{23}c_{12}^2 s_{13}s_{23}\cos\left(\delta_{\text{CP}} + \xi_3\right) - c_{23}s_{12}^2 s_{13}s_{23}\cos\left(\delta_{\text{CP}} - \xi_3\right)\right. \\
& \qquad \left. + c_{12}s_{12}\left(c_{23}^2 - s_{13}^2 s_{23}^2\right)\cos\xi_3\right] \\
& + 2\,|\Lambda_1\Lambda_3| \left[c_{13}s_{23}\left(c_{12}s_{13}s_{23}\cos\left(\delta_{\text{CP}} - \xi_2\right) + c_{23}s_{12}\cos\xi_2\right)\right] \\
& + 2\,|\Lambda_2\Lambda_3| \left[c_{13}s_{23}\left(s_{12}s_{13}s_{23}\cos\left(\delta_{\text{CP}} - \xi_1\right) - c_{12}c_{23}\cos\xi_1\right)\right] .
\end{aligned}$$

[Miranda, DKP, Tórtola, Valle, JHEP 1907 (2019) 103]

TMMs in flavor & mass basis @ SNS facilities (delayed ν_e)

Delayed beam: (i) ν_e (with $\mathfrak{a}_-^1 = 1$) and (ii) $\bar{\nu}_\mu$ (with $\mathfrak{a}_+^2 = 1$)

ν_e component

- flavor basis

$$\left(\mu^F_{\nu_e,\,\text{delayed}}\right)^2 = |\Lambda_\mu|^2 + |\Lambda_\tau|^2$$

- mass basis

$$\begin{aligned}\left(\mu^M_{\nu_e,\,\text{delayed}}\right)^2 =& |\Lambda_1|^2 \left[c_{13}^2 s_{12}^2 + s_{13}^2\right] + |\Lambda_2|^2 \left[c_{12}^2 c_{13}^2 + s_{13}^2\right] + |\Lambda_3|^2\, c_{13}^2 \\ &- |\Lambda_1 \Lambda_2| \left[c_{13}^2 \sin(2\theta_{12}) \cos\xi_3\right] - |\Lambda_1 \Lambda_3| \left[c_{12} \sin(2\theta_{13}) \cos(\delta_{\text{CP}} - \xi_2)\right] \\ &- |\Lambda_2 \Lambda_3| \left[s_{12} \sin(2\theta_{13}) \cos(\delta_{\text{CP}} - \xi_1)\right] ,\end{aligned}$$

[Miranda, DKP, Tórtola, Valle, JHEP 1907 (2019) 103]

TMMs in flavor & mass basis @ SNS facilities (delayed $\bar{\nu}_\mu$)

Delayed beam: (i) ν_e (with $\mathfrak{a}_-^1 = 1$) and (ii) $\bar{\nu}_\mu$ (with $\mathfrak{a}_+^2 = 1$)

$\bar{\nu}_\mu$ component

- flavor basis

$$\left(\mu^F_{\bar{\nu}_\mu,\,\text{delayed}}\right)^2 = |\Lambda_e|^2 + |\Lambda_\tau|^2$$

- mass basis

$$\begin{aligned}
\left(\mu^M_{\bar{\nu}_\mu,\,\text{delayed}}\right)^2 = {} & |\Lambda_1|^2 \left[-2c_{12}c_{23}s_{12}s_{13}s_{23}\cos\delta_{\text{CP}} + s_{23}^2\left(c_{13}^2 + s_{12}^2 s_{13}^2\right) + c_{12}^2 c_{23}^2\right] \\
& + |\Lambda_2|^2 \left[2c_{12}c_{23}s_{12}s_{13}s_{23}\cos\delta_{\text{CP}} + s_{23}^2\left(c_{13}^2 + c_{12}^2 s_{13}^2\right) + s_{12}^2 c_{23}^2\right] \\
& + |\Lambda_3|^2 \left[\frac{1}{4}\left(2c_{13}^2\cos(2\theta_{23}) - \cos(2\theta_{13}) + 3\right)\right] \\
& + 2\,|\Lambda_1\Lambda_2| \left[c_{23}s_{13}s_{23}\left(c_{12}^2\cos\left(\delta_{\text{CP}} + \xi_3\right) - s_{12}^2\cos\left(\delta_{\text{CP}} - \xi_3\right)\right)\right. \\
& \left. + c_{12}c_{23}^2 s_{12}\cos\xi_3 - c_{12}s_{12}s_{13}^2 s_{23}^2\cos\xi_3\right] \\
& + 2\,|\Lambda_1\Lambda_3| \left[c_{13}s_{23}\left(c_{12}s_{13}s_{23}\cos\left(\delta_{\text{CP}} - \xi_2\right) + c_{23}s_{12}\cos\xi_2\right)\right] \\
& + 2\,|\Lambda_2\Lambda_3| \left[c_{13}s_{23}\left(s_{12}s_{13}s_{23}\cos\left(\delta_{\text{CP}} - \xi_1\right) - c_{12}c_{23}\cos\xi_1\right)\right]
\end{aligned}$$

[Miranda, DKP, Tórtola, Valle, JHEP 1907 (2019) 103]

Analysis of CEνNS data: sensitivity to $|\Lambda_i|$

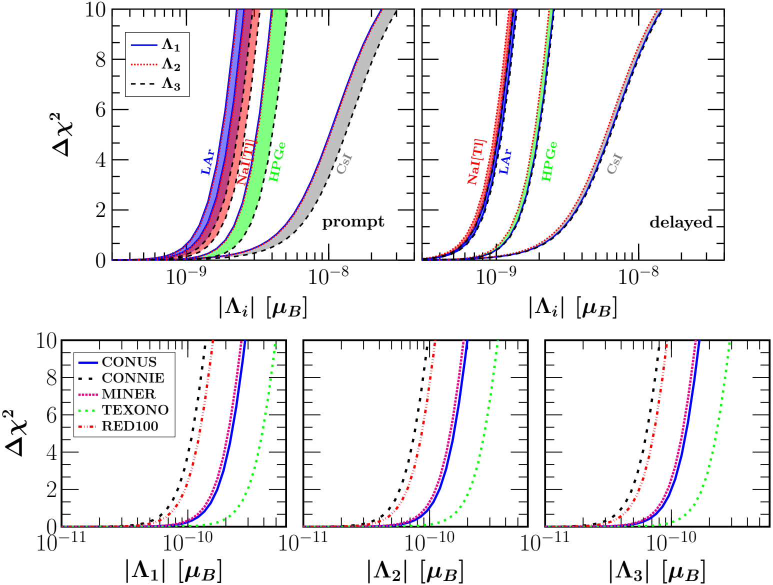

all results in units $10^{-10}\mu_B$

[Miranda, DKP, Tórtola, Valle, JHEP 1907 (2019) 103]

Estimating the future prospects: luminosity factor variation

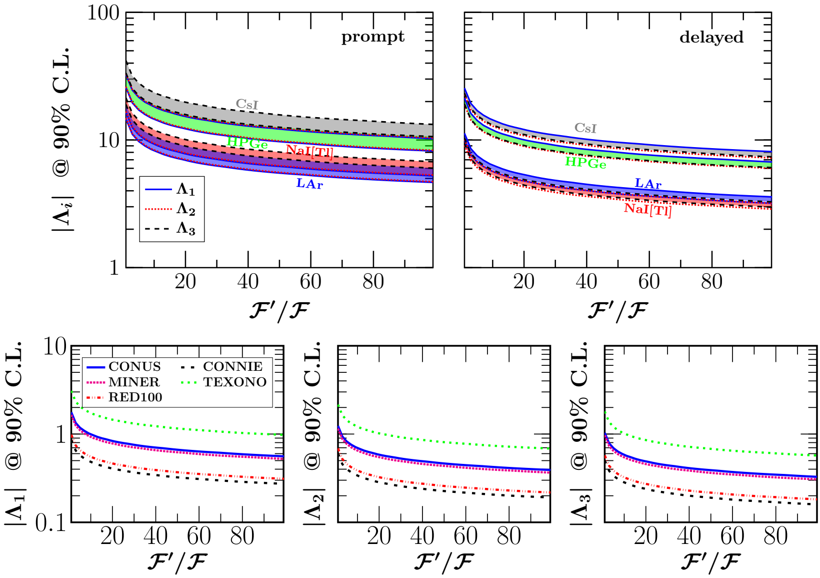

all results in units $10^{-10}\mu_B$

[Miranda, DKP, Tórtola, Valle, JHEP 1907 (2019) 103]

Current COHERENT setup: combined constraints

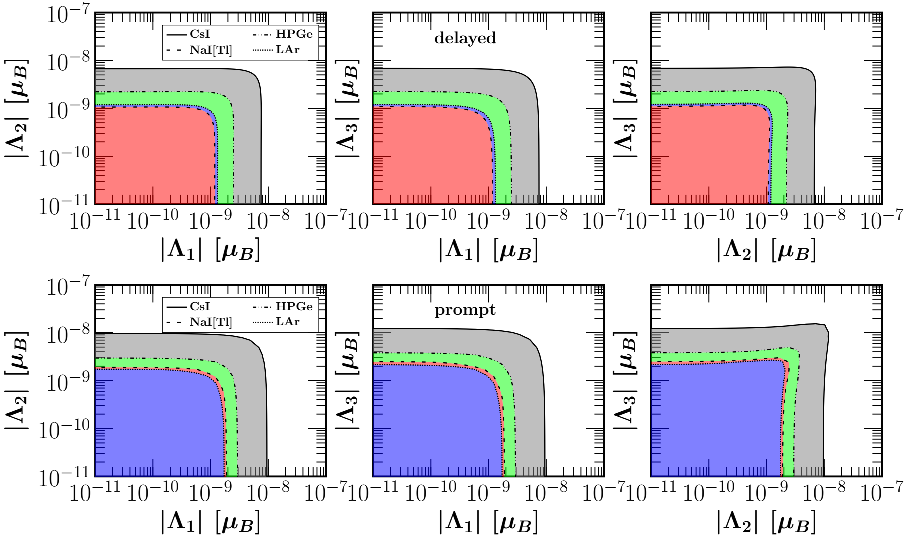

[Miranda, DKP, Tórtola, Valle, JHEP 1907 (2019) 103]

Current & Future Reactor experiments: combined constraints

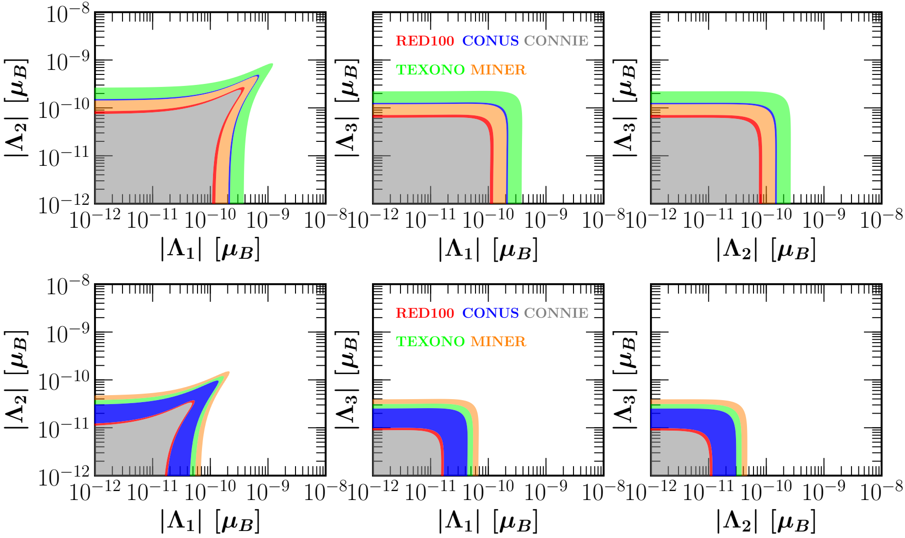

[Miranda, DKP, Tórtola, Valle, JHEP 1907 (2019) 103]

Solar neutrinos from Borexino

[Miranda, DKP, Tórtola, Valle, JHEP 1907 (2019) 103]

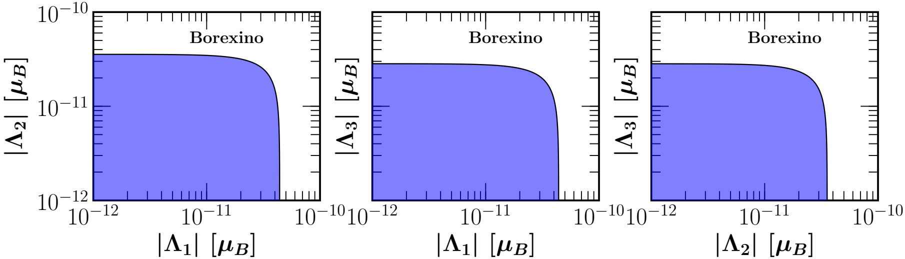

- solar electron neutrinos undergo flavor oscillations arriving to the detector as an incoherent admixture of mass eigenstates (no phase dependence)
- dependence on neutrino mixing and oscillation factor between the source and detection is considered $\left(\mu^M_{\nu,\text{eff}}\right)^2(L, E_\nu) = \sum_j \left| \sum_i U^*_{\alpha i} e^{-i\,\Delta m^2_{ij} L/2E_\nu} \tilde{\lambda}_{ij} \right|^2$
- the oscillation probabilities from ν_e to mass eigenstates ν_i are approximated

$$P^{3\nu}_{e3} = \sin^2\theta_{13}, \quad P^{3\nu}_{e1} = \cos^2\theta_{13} P^{2\nu}_{e1}, \quad P^{3\nu}_{e2} = \cos^2\theta_{13} P^{2\nu}_{e2},$$

  and the unitarity condition, $P^{2\nu}_{e1} + P^{2\nu}_{e2} = 1$
- eff. neutrino magnetic moment for solar neutrinos in mass basis [Cañas et al.: PLB 753 (2016)]

$$(\mu^M_{\nu,\,\text{sol}})^2 = |\mathbf{\Lambda}|^2 - c^2_{13}|\Lambda_2|^2 + (c^2_{13} - 1)|\Lambda_3|^2 + c^2_{13} P^{2\nu}_{e1}(|\Lambda_2|^2 - |\Lambda_1|^2)$$

- Recall Borexino phase-II limit $\mu_\nu < 2.8 \times 10^{-11} \mu_B$ [Borexino Collab., Agostini et al.:PRD 96 (2017)]

Impact of CP phases

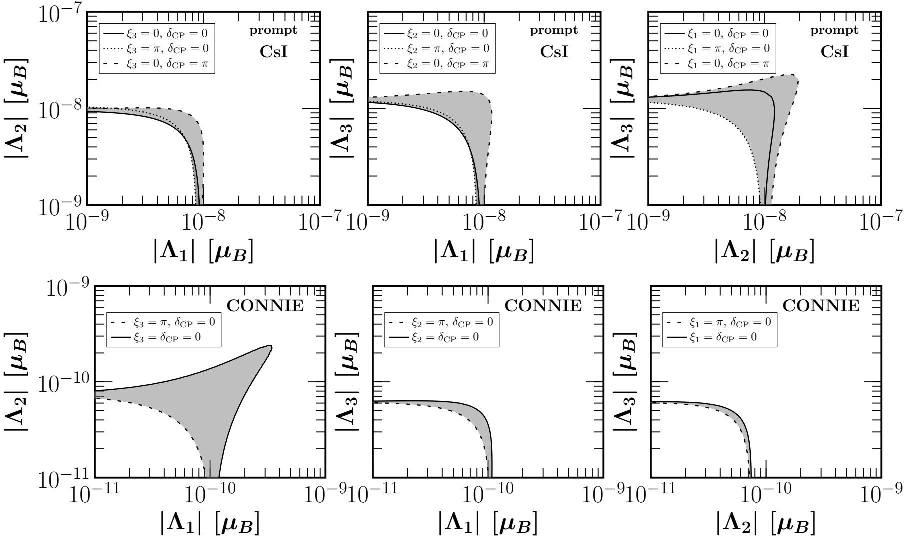

explore the robustness of TMMs limits [Miranda, DKP, Tórtola, Valle, JHEP 1907 (2019) 103]

Sterile neutrinos & violation of lepton unitarity

Sensitivity to the sterile mixing parameters (COHERENT)

- **Matrix elements in the (3+1) scheme**

  $|U_{e4}|^2 = s_{14}^2,\ |U_{\mu 4}|^2 = s_{24}^2 c_{14}^2,$

  $s_{ij} \equiv \sin\phi_{ij}$ and $c_{ij} \equiv \cos\phi_{ij}$

- **Mixing angles**

$$\sin^2 2\theta_{\alpha\alpha} = 4|U_{\alpha 4}|^2(1-|U_{\alpha 4}|^2)$$
$$\sin^2 2\theta_{\alpha\beta} = 4|U_{\alpha 4}|^2|U_{\beta 4}|^2$$

- **Oscillation probability**

$$P_{\alpha\beta} \approx = \begin{cases} 1-\sin^2 2\theta_{\alpha\alpha}\sin^2\frac{\Delta_{41}}{2} & (\alpha=\beta) \\ \sin^2 2\theta_{\alpha\beta}\sin^2\frac{\Delta_{41}}{2} & (\alpha\neq\beta) \end{cases},$$

$\Delta_{ij} \equiv 2.54\left(\Delta m_{ij}^2/\mathrm{eV}^2\right)(L/\mathrm{km})(\mathrm{GeV}/E_\nu),$

where $\Delta m_{ij}^2 \equiv m_i^2 - m_j^2$

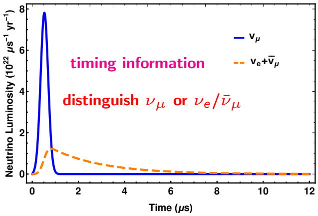

- **exclusion curves: 100 kg CsI, 3 years**
  [Blanco, Hooper, Machado arXiv:1901.08094]

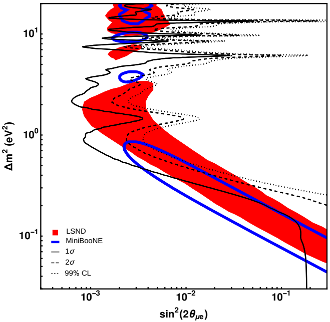

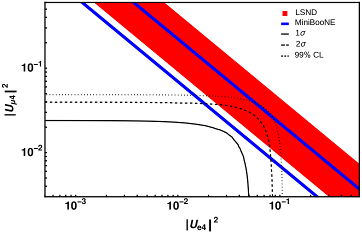

Sensitivity to the sterile mixing parameters (reactors)

- **Matrix elements in the (3+1) scheme**

  $|U_{e4}|^2 = s_{14}^2, \, |U_{\mu 4}|^2 = s_{24}^2 c_{14}^2,$
  $s_{ij} \equiv \sin\phi_{ij}$ and $c_{ij} \equiv \cos\phi_{ij}$

- **Mixing angles**

$$\sin^2 2\theta_{\alpha\alpha} = 4|U_{\alpha 4}|^2(1 - |U_{\alpha 4}|^2)$$
$$\sin^2 2\theta_{\alpha\beta} = 4|U_{\alpha 4}|^2|U_{\beta 4}|^2$$

- **Oscillation probability**

$$P_{\alpha\beta} \approx = \begin{cases} 1 - \sin^2 2\theta_{\alpha\alpha} \sin^2 \frac{\Delta_{41}}{2} & (\alpha = \beta) \\ \sin^2 2\theta_{\alpha\beta} \sin^2 \frac{\Delta_{41}}{2} & (\alpha \neq \beta) \end{cases} ,$$

  $\Delta_{ij} \equiv 2.54 \left(\Delta m_{ij}^2/\mathrm{eV}^2\right)(L/\mathrm{km})(\mathrm{GeV}/E_\nu),$
  where $\Delta m_{ij}^2 \equiv m_i^2 - m_j^2$

- **exclusion curves: reactor CEνNS experiments**
  [Berryman PRD D100 (2019) 023540]

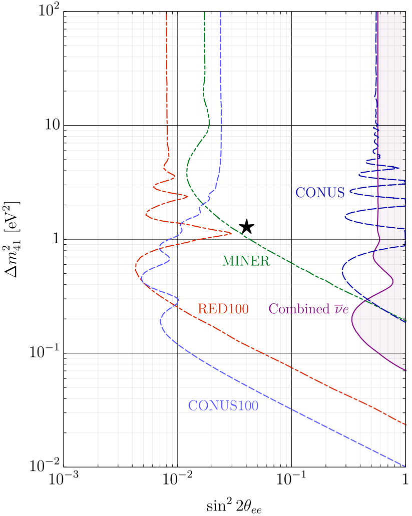

Future sensitivities at π-DAR sources

[Miranda, DKP, Sanders, Tórtola, Valle, PRD 102 (2020) 113014]

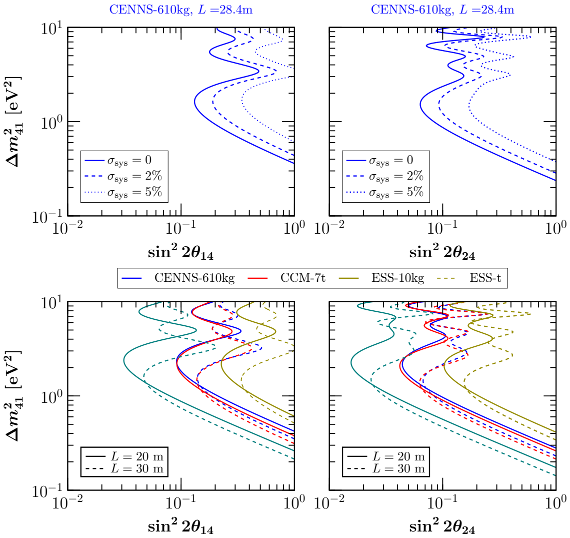

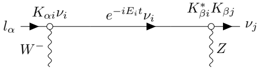

survival probability

$$P_\alpha = \sum_{i,l,\beta} K_{\alpha i} e^{-iE_i t} K^*_{\beta i} K_{\beta l} e^{iE_l t} K^*_{\alpha l}$$

Non-unitary (NU) neutrino mixing: general case

- Assume: extra singlet neutral heavy leptons that mediate light-neutrino mass generation.
- Goal: to constrain the non-unitarity parameters through neutral current.
- The generalized charged current weak interaction mixing matrix reads $N = N^{\mathrm{NP}} U^{3\times 3}$ with

$$N^{\mathrm{NP}} = \begin{pmatrix} \alpha_{11} & 0 & 0 \\ \alpha_{21} & \alpha_{22} & 0 \\ \alpha_{31} & \alpha_{32} & \alpha_{33} \end{pmatrix},$$

  with the diagonal (off-diagonal) components α_{ii} (α_{ij}) being real (complex) numbers.
- modifications in oscillation pattern

$$P_{\alpha\beta} = \sum_{i,j}^{3} N^*_{\alpha i} N_{\beta i} N_{\alpha j} N^*_{\beta j} - 4 \sum_{j>i}^{3} Re\left[N^*_{\alpha j} N_{\beta j} N_{\alpha i} N^*_{\beta i}\right] \sin^2\left(\frac{\Delta m^2_{ji} L}{4E_\nu}\right)$$
$$+2 \sum_{j>i}^{3} Im\left[N^*_{\alpha j} N_{\beta j} N_{\alpha i} N^*_{\beta i}\right] \sin\left(\frac{\Delta m^2_{ji} L}{2E_\nu}\right).$$

[Escrihuela, Forero, Miranda, Tortola, Valle, PRD 92 5, 053009]

Non-unitary (NU) neutrino mixing: CEvNS experiments

For the short-baseline CEvNS experiments we are interested in here, there is no time for oscillations among active neutrinos to develop.

$$\begin{aligned} P_{ee} &= \alpha_{11}^4, \\ P_{\mu\mu} &= (|\alpha_{21}|^2 + \alpha_{22}^2)^2, \\ P_{\mu e} &= \alpha_{11}^2 |\alpha_{21}|^2, \\ P_{e\tau} &= \alpha_{11}^2 |\alpha_{31}|^2, \\ P_{\mu\tau} &\simeq \alpha_{22}^2 |\alpha_{32}|^2, \end{aligned} \tag{3}$$

while the following "triangle inequalities" among the elements of the N^{NP} matrix hold

$$\begin{aligned} |\alpha_{21}| &\leq \sqrt{(1-\alpha_{11}^2)(1-\alpha_{22}^2)}\,, \\ |\alpha_{31}| &\leq \sqrt{(1-\alpha_{11}^2)(1-\alpha_{33}^2)}\,, \\ |\alpha_{32}| &\leq \sqrt{(1-\alpha_{22}^2)(1-\alpha_{33}^2)}\,. \end{aligned}$$

[Escrihuela, Forero, Miranda, Tortola, Valle, PRD 92 5, 053009]

Modification of neutrino spectra

Due to the zero-distance effect the neutrino spectra at the detector are:

$$\begin{pmatrix} \frac{\mathrm{d}\phi_e^{\mathrm{NU}}}{\mathrm{d}E_\nu} \\ \frac{\mathrm{d}\phi_\mu^{\mathrm{NU}}}{\mathrm{d}E_\nu} \\ \frac{\mathrm{d}\phi_\tau^{\mathrm{NU}}}{\mathrm{d}E_\nu} \end{pmatrix} = \begin{pmatrix} P_{ee} & P_{\mu e} & P_{\tau e} \\ P_{e\mu} & P_{\mu\mu} & P_{\tau\mu} \\ P_{e\tau} & P_{\mu\tau} & P_{\tau\tau} \end{pmatrix} \begin{pmatrix} \frac{\mathrm{d}\phi_{\nu_e}^0}{\mathrm{d}E_\nu} \\ \frac{\mathrm{d}\phi_{\nu_\mu}^0}{\mathrm{d}E_\nu} \\ \frac{\mathrm{d}\phi_{\nu_\tau}^0}{\mathrm{d}E_\nu} \end{pmatrix} + \begin{pmatrix} \overline{P_{ee}} & \overline{P_{\mu e}} & \overline{P_{\tau e}} \\ \overline{P_{e\mu}} & \overline{P_{\mu\mu}} & \overline{P_{\tau\mu}} \\ \overline{P_{e\tau}} & \overline{P_{\mu\tau}} & \overline{P_{\tau\tau}} \end{pmatrix} \begin{pmatrix} \frac{\mathrm{d}\phi_{\bar\nu_e}^0}{\mathrm{d}E_\nu} \\ \frac{\mathrm{d}\phi_{\bar\nu_\mu}^0}{\mathrm{d}E_\nu} \\ \frac{\mathrm{d}\phi_{\bar\nu_\tau}^0}{\mathrm{d}E_\nu} \end{pmatrix} .$$

with $\overline{P_{\alpha\beta}} = P(\overline{\nu}_\alpha \to \overline{\nu}_\beta)$.

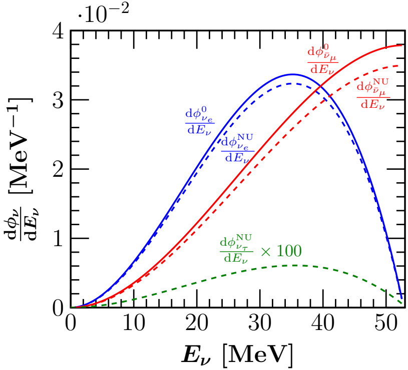

Miranda, DKP, Sanders, Tórtola, Valle, PRD 102 (2020) 113014

Sensitivity on NU parameters

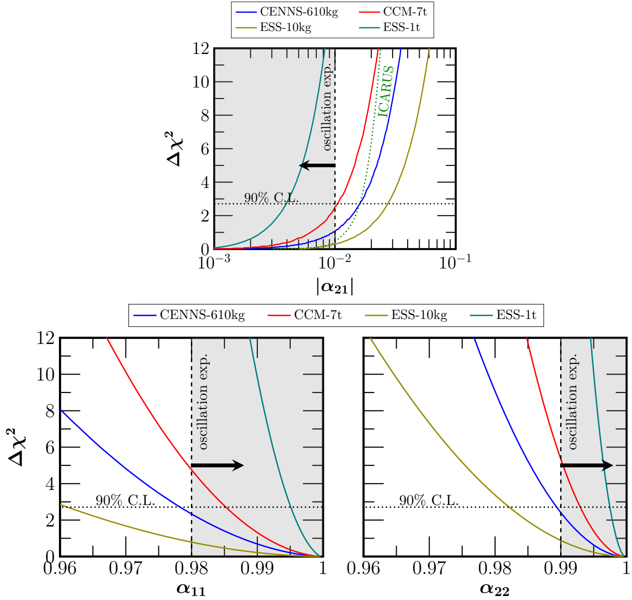

Miranda, DKP, Sanders, Tórtola, Valle, PRD 102 (2020) 113014

Sensitivity on NU parameters

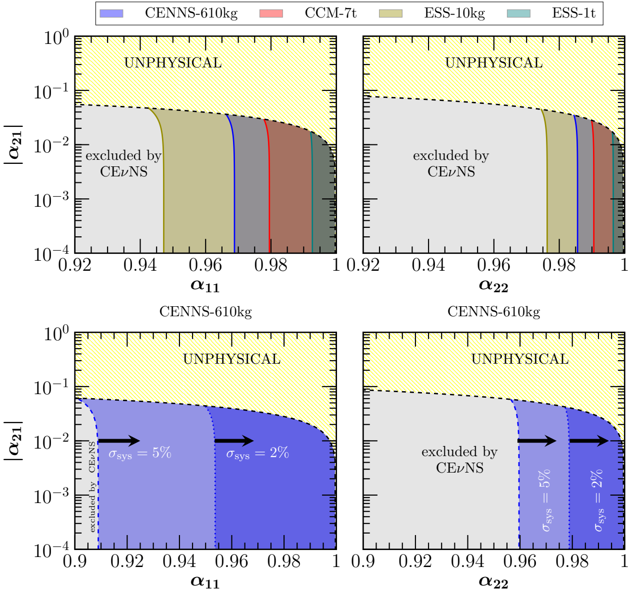

Miranda, DKP, Sanders, Tórtola, Valle, PRD 102 (2020) 113014

WIMP-nucleus scattering & the neutrino floor

Neutrino Backgrounds to Dark Matter Searches

- Solar neutrinos
  W. C. Haxton, R. G. Hamish Robertson, and A. M. Serenelli, Ann. Rev. Astron. Astrophys. **51** (2013), 21
- Low-energy Atmospheric neutrinos (FLUKA simulations)
  G. Battistoni, A. Ferrari, T. Montaruli, and P. R. Sala, Astropart. Phys. **23** (2005) 526
- Diffuse Supernova neutrinos S. Horiuchi, J. F. Beacom, and E. Dwek, Phys. Rev. **D79** (2009) 083013

type	$E_{\nu_{\max}}$ [MeV]	flux $[\mathrm{cm}^{-2}\mathrm{s}^{-1}]$
pp	0.423	$(5.98 \pm 0.006) \times 10^{10}$
pep	1.440	$(1.44 \pm 0.012) \times 10^{8}$
hep	18.784	$(8.04 \pm 1.30) \times 10^{3}$
$^{7}\mathrm{Be}_{\mathrm{low}}$	0.3843	$(4.84 \pm 0.48) \times 10^{8}$
$^{7}\mathrm{Be}_{\mathrm{high}}$	0.8613	$(4.35 \pm 0.35) \times 10^{9}$
$^{8}\mathrm{B}$	16.360	$(5.58 \pm 0.14) \times 10^{6}$
$^{13}\mathrm{N}$	1.199	$(2.97 \pm 0.14) \times 10^{8}$
$^{15}\mathrm{O}$	1.732	$(2.23 \pm 0.15) \times 10^{8}$
$^{17}\mathrm{F}$	1.740	$(5.52 \pm 0.17) \times 10^{6}$

Solar neutrino fluxes and uncertainties in the framework of the employed high metallicity SSM

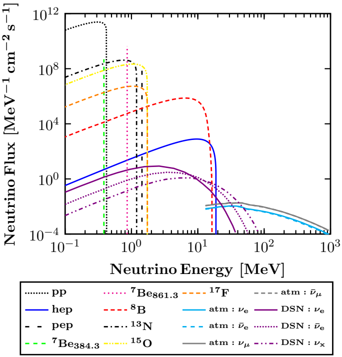

Astroneutrino-induced events at Dark Matter detectors

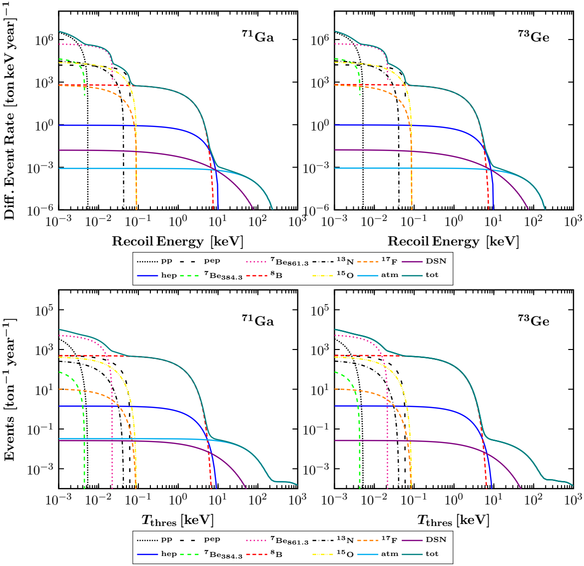

[DKP, Sahu, Kosmas, Kota, Nayak Adv.High Energy Phys. 2018 (2018) 6031362]

Incoherent vs. Coherent rates: solar neutrinos

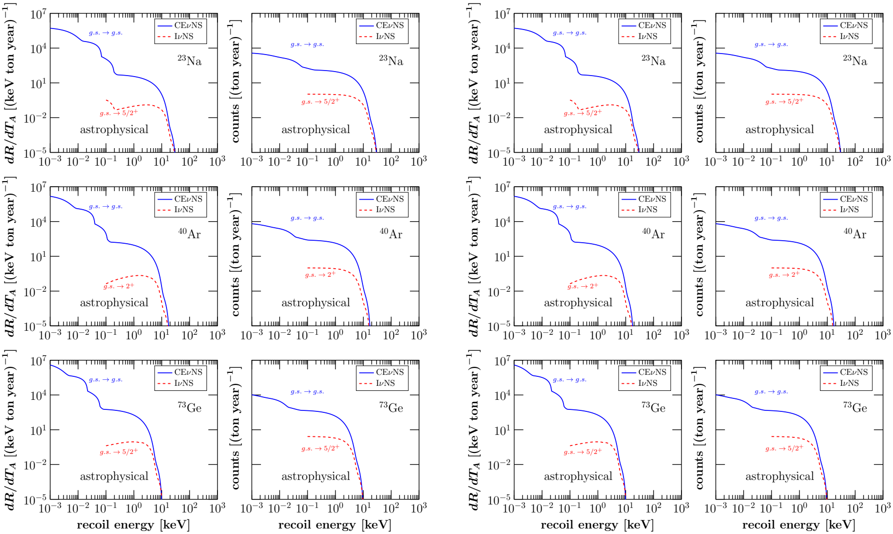

[Sahu, DKP, Kota, Kosmas, PRC 102 (2020) 3, 035501]

Astro-neutrino events in the presence of new physics

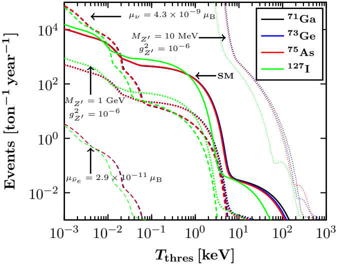

[DKP, Sahu, Kosmas, Kota, Nayak Adv.High Energy Phys. 2018 (2018) 6031362]

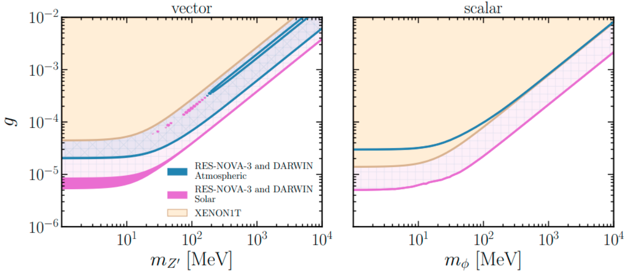

[Suliga, Tamborra PRD 103, 083002 (2021)]

WIMP-nucleus cross section

- Cross section in lab. frame

$$\frac{d\sigma(u,\upsilon)}{du} = \frac{1}{2}\sigma_0\left(\frac{1}{m_p b}\right)^2 \frac{c^2}{\upsilon^2}\frac{d\sigma_A(u)}{du},$$

- spin dependent/coherent

$$\frac{d\sigma_A}{du} = \left[f_A^0\Omega_0(0)\right]^2 F_{00}(u) + 2f_A^0 f_A^1\Omega_0(0)\Omega_1(0)F_{01}(u) + \left[f_A^1\Omega_1(0)\right]^2 F_{11}(u) + \mathcal{M}^2(u).$$

$$\mathcal{M}^2(u) = (f_S^0\,[ZF_Z(u)+NF_N(u)] + f_S^1\,[ZF_Z(u)-NF_N(u)])^2.$$

- model dependent parameters
f_A^0, f_A^1 for the isoscalar and isovector parts of the axial-vector current
f_S^0, f_S^1 for the isoscalar and isovector parts of the scalar current

- Spin structure coefficients

$$F_{\rho\rho'}(u) = \sum_{\lambda,\kappa}\frac{\Omega_\rho^{(\lambda,\kappa)}(u)\Omega_{\rho'}^{(\lambda,\kappa)}(u)}{\Omega_\rho(0)\Omega_{\rho'}(0)}$$

contributions
with $\rho,\ \rho' = 0, 1$ for the isoscalar and isovector

$$\Omega_\rho^{(\lambda,\kappa)}(u) = \sqrt{\frac{4\pi}{2J_i+1}} \times \langle J_f||\sum_{j=1}^{A}\left[Y_\lambda(\Omega_j)\otimes\sigma(j)\right]_\kappa j_\lambda(\sqrt{u}\,r_j)\omega_\rho(j)||J_i\rangle.$$

$\omega_0(j) = 1$ and $\omega_1(j) = \tau(j)$ with $\tau = +1(-1)$ for protons (neutrons)
Ω_j: solid angle for the position vector of the j-th nucleon.

- evaluation of the reduced nuclear matrix element
(first calculate the single particle matrix elements)

$$\langle n_i l_i j_i||\hat{t}^{(l,s)J}||n_k l_k j_k\rangle = \sqrt{(2j_k+1)(2j_i+1)(2J+1)(s+1)(s+2)} \times \left\{\begin{array}{ccc} l_i & 1/2 & j_i \\ l_k & 1/2 & j_k \\ l & s & J\end{array}\right\}\langle l_i||\sqrt{4\pi}\,Y^l||l_k\rangle\,\langle n_i l_i|j_l(kr)|n_l l_k\rangle$$

DKP et al., Adv.High Energy Phys. 2018 (2018) 6031362

WIMP-nucleus cross section

- Cross section in lab. frame

$$\frac{d\sigma(u,\upsilon)}{du} = \frac{1}{2}\sigma_0 \left(\frac{1}{m_p b}\right)^2 \frac{c^2}{\upsilon^2}\frac{d\sigma_A(u)}{du} ,$$

- spin dependent/coherent

$$\frac{d\sigma_A}{du} = \left[f_A^0 \Omega_0(0)\right]^2 F_{00}(u) + 2 f_A^0 f_A^1 \Omega_0(0)\Omega_1(0) F_{01}(u) + \left[f_A^1 \Omega_1(0)\right]^2 F_{11}(u) + \mathcal{M}^2(u) .$$

$$\mathcal{M}^2(u) = (f_S^0 \left[Z F_Z(u) + N F_N(u)\right] + f_S^1 \left[Z F_Z(u) - N F_N(u)\right])^2 .$$

- model dependent parameters

f_A^0, f_A^1 for the isoscalar and isovector parts of the axial-vector current

f_S^0, f_S^1 for the isoscalar and isovector parts of the scalar current

- Spin structure coefficients

$$F_{\rho\rho'}(u) = \sum_{\lambda,\kappa} \frac{\Omega_\rho^{(\lambda,\kappa)}(u)\Omega_{\rho'}^{(\lambda,\kappa)}(u)}{\Omega_\rho(0)\Omega_{\rho'}(0)}$$

contributions
with $\rho,\ \rho' = 0, 1$ for the isoscalar and isovector

$$\Omega_\rho^{(\lambda,\kappa)}(u) = \sqrt{\frac{4\pi}{2J_i + 1}} \times \langle J_f || \sum_{j=1}^{A} \left[Y_\lambda(\Omega_j) \otimes \sigma(j)\right]_\kappa j_\lambda(\sqrt{u}\, r_j)\omega_\rho(j) || J_i \rangle .$$

$\omega_0(j) = 1$ and $\omega_1(j) = \tau(j)$ with $\tau = +1(-1)$ for protons (neutrons)

Ω_j: solid angle for the position vector of the j-th nucleon.

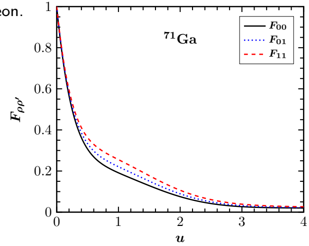

DKP et al., Adv.High Energy Phys. 2018 (2018) 6031362

WIMP-nucleus scattering: nuclear physics corrections

The normalized spin structure functions $F_{\rho\rho'}(u)$ with $\rho,\ \rho' = 0{,}1$ are defined as

$$F_{\rho\rho'}(u) = \sum_{\lambda,\kappa} \frac{\Omega_\rho^{(\lambda,\kappa)}(u)\Omega_{\rho'}^{(\lambda,\kappa)}(u)}{\Omega_\rho \Omega_{\rho'}}$$

$$\Omega_\rho^{(\lambda,\kappa)}(u) = \sqrt{\frac{4\pi}{2J_i+1}} \times \langle J_f \| \sum_{j=1}^{A} \left[Y_\lambda(\Omega_j) \otimes \sigma(j) \right]_\kappa j_\lambda(\sqrt{u}\, r_j)\omega_\rho(j) \| J_i \rangle \,,$$

- $\omega_0(j) = 1$ and $\omega_1(j) = \tau(j)$ with $\tau = +1$ for protons and $\tau = -1$ for neutrons
- j_λ is the spherical Bessel function
- the static spin matrix elements are defined as $\Omega_\rho(0) = \Omega_\rho^{(0,1)}(0)$

elastic scattering

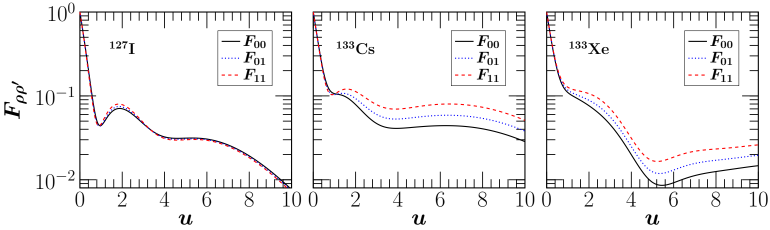

[Sahu, DKP, Kota, Kosmas, PRC 102 (2020) 3, 035501]

WIMP-nucleus scattering: nuclear physics corrections

The normalized spin structure functions $F_{\rho\rho'}(u)$ with ρ, $\rho' = 0{,}1$ are defined as

$$F_{\rho\rho'}(u) = \sum_{\lambda,\kappa} \frac{\Omega_{\rho}^{(\lambda,\kappa)}(u)\Omega_{\rho'}^{(\lambda,\kappa)}(u)}{\Omega_{\rho}\Omega_{\rho'}}$$

$$\Omega_{\rho}^{(\lambda,\kappa)}(u) = \sqrt{\frac{4\pi}{2J_i+1}} \times \langle J_f \| \sum_{j=1}^{A} \left[Y_{\lambda}(\Omega_j) \otimes \sigma(j) \right]_{\kappa} j_{\lambda}(\sqrt{u}\, r_j)\omega_{\rho}(j) \| J_i \rangle \,,$$

- $\omega_0(j) = 1$ and $\omega_1(j) = \tau(j)$ with $\tau = +1$ for protons and $\tau = -1$ for neutrons
- j_{λ} is the spherical Bessel function
- the static spin matrix elements are defined as $\Omega_{\rho}(0) = \Omega_{\rho}^{(0,1)}(0)$

inelastic scattering

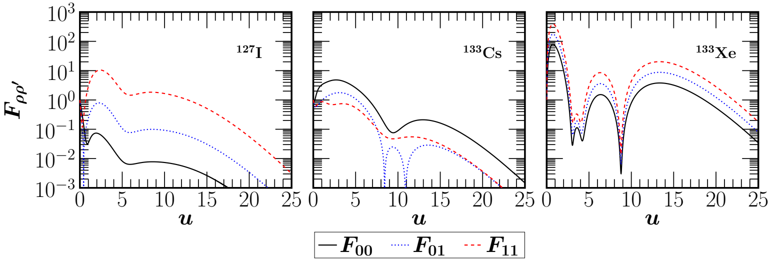

[Sahu, DKP, Kota, Kosmas, PRC 102 (2020) 3, 035501]

WIMP-nucleus rates

- differential WIMP-nucleus event rate

$$\frac{dR(u,\upsilon)}{dq^2} = N_t \phi \frac{d\sigma}{dq^2} f(\upsilon)\, d^3\upsilon, \quad \phi = \rho_0 \upsilon / m_\chi$$

with the dimensional parameter $u = q^2 b^2/2$

ρ_0 is the local WIMP density

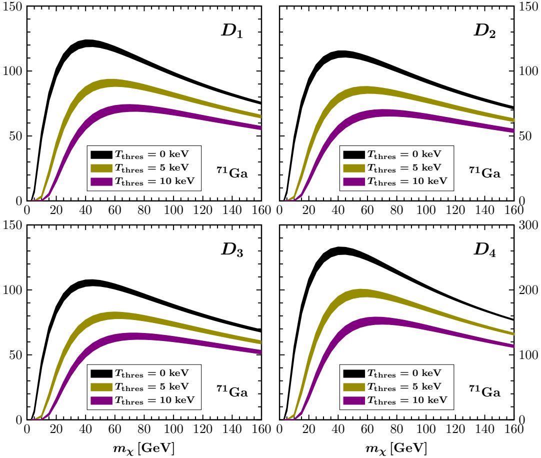

- $f(\upsilon)$: distribution of WIMP velocity (Maxwell-Boltzmann)

for consistency with the LSP

- WIMP-nucleus rate

$$\langle R \rangle = (f_A^0)^2 D_1 + 2 f_A^0 f_A^1 D_2 + (f_A^1)^2 D_3 + A^2 \left(f_S^0 - f_S^1 \frac{A-2Z}{A} \right)^2 |F(u)|^2 D_4 \, .$$

with

$$D_i = \int_{-1}^{1} d\xi \int_{\psi_{\rm min}}^{\psi_{\rm max}} d\psi \int_{u_{\rm min}}^{u_{\rm max}} G(\psi,\xi) X_i \, du \, ,$$

and

$$X_1 = [\Omega_0(0)]^2 \, F_{00}(u) \, ,$$
$$X_2 = \Omega_0(0)\Omega_1(0) F_{01}(u) \, ,$$
$$X_3 = [\Omega_1(0)]^2 \, F_{11}(u) \, ,$$
$$X_4 = |F(u)|^2 \, .$$

DKP et al., Adv.High Energy Phys. 2018 (2018) 6031362

Elastic WIMP Event Rates

$$\langle R \rangle_{\rm el} = \int_{-1}^{1} d\xi \int_{\psi_{min}}^{\psi_{max}} d\psi \int_{u_{min}}^{u_{max}} G(\psi,\xi) \frac{d\sigma_A(u)}{du} du \,.$$

where [Pirinen, Srivastava, Suhonen, Kortelainen PRD 93, 095012]

$$G(\psi,\xi) = \frac{\rho_0}{m_\chi} \frac{\sigma_0}{Am_p} \left(\frac{1}{m_p b}\right)^2 \frac{c^2}{\sqrt{\pi} v_0} \psi e^{-\lambda^2} e^{-\psi^2} e^{-2\lambda\psi\xi} \,, \text{ with } \psi = v/v_0,\ \lambda = v_E/v_0,\ \xi = \cos(\theta).$$

Integration limits

$$\psi_{\rm min} = \frac{c}{v_0} \left(\frac{Am_p T_{\rm thres}}{2\mu_r^2} \right)^{1/2} , \qquad \psi_{\rm max} = -\lambda\xi + \sqrt{\lambda^2\xi^2 + \frac{v_{esc}^2}{v_0^2} - 1 - \frac{v_1^2}{v_0^2} - \frac{2v_1}{v_0}\sin(\gamma)\cos(\alpha)} \,,$$

$$u_{\rm min} = Am_p T_{\rm thres} b^2 \,, \qquad u_{\rm max} = 2(\psi \mu_r b v_0/c)^2 \,.$$

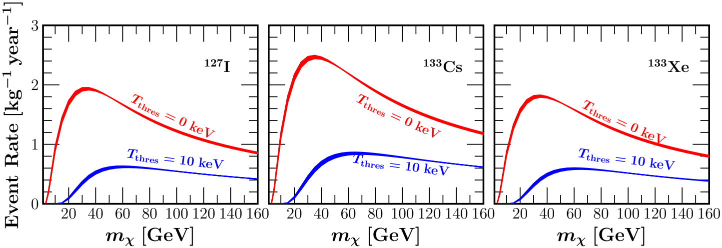

[Sahu, DKP, Kota, Kosmas, PRC 102 (2020) 3, 035501]

Inelastic WIMP Event Rates

$$\langle R \rangle_{\text{inel}} = (f_1^0)^2 E_1 + 2 f_A^0 f_A^1 E_2 + (f_A^1)^2 E_3 \,,$$

where E_1, E_2 and E_3 are the three dimensional integrals

$$E_i = \int_{-1}^{1} d\xi \int_{\psi_{\text{min}}}^{\psi_{\text{max}}} d\psi \int_{u_{\text{min}}}^{u_{\text{max}}} G(\psi, \xi) X(i) \, du \,.$$

The integration limits read [Pirinen, Srivastava, Suhonen, Kortelainen PRD 93, 095012]

$$u_{\text{min}} = \frac{1}{2} b^2 \mu_r^2 \frac{v_0^2}{c^2} \psi^2 \left[1 - \sqrt{1 - \frac{\Gamma}{\psi^2}} \right]^2 , \qquad u_{\text{max}} = \frac{1}{2} b^2 \mu_r^2 \frac{v_0^2}{c^2} \psi^2 \left[1 + \sqrt{1 - \frac{\Gamma}{\psi^2}} \right]^2 ,$$

where

$$\Gamma = \frac{2E^*}{\mu_r c^2} \frac{c^2}{v_0^2} \,, \quad \text{E}^* \text{ is the excitation energy}$$

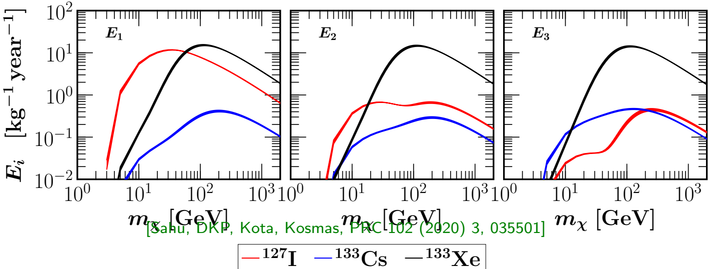

[Sahu, DKP, Kota, Kosmas, PRC 102 (2020) 3, 035501]

The neutrino floor

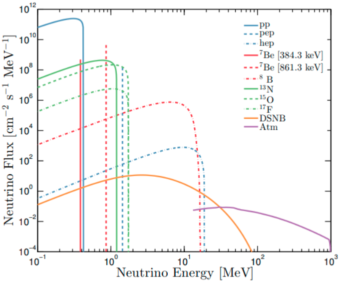

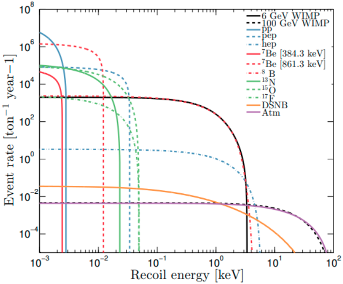

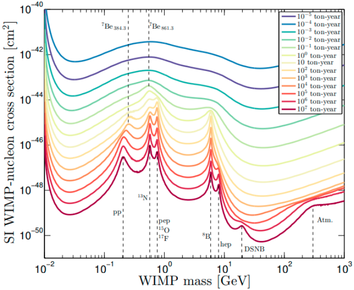

O'Hare PRD 94, 063527 (2016)

The neutrino floor: uncertainties

Signal — Uncertainties — Background

Astrophysical uncertainties
O'Hare [1604.03858]

Astrophysical uncertainty in DM $f(v)$

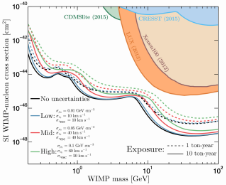

Nuclear physics uncertainties
Papoulias et al. [1804.11319]

Nuclear form factors for DM / CEvNS

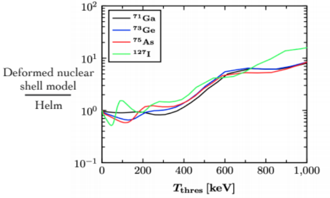

Non-standard interactions
Aristizabal Sierra et al. [1712.09667]

Gonzalez-Garcia et al. [1803.03650]

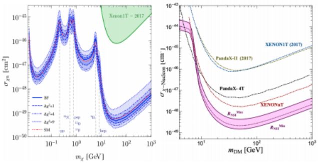

New mediators
Boehm et al. [1809.06385]

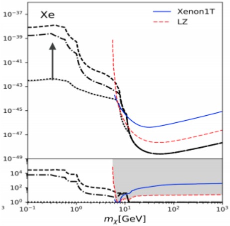

Summary

SM CEνNS reaction (conventional)

$$\nu_\alpha + (A, Z) \rightarrow \nu_\alpha + (A, Z), \quad \alpha = (e, \mu, \tau)$$

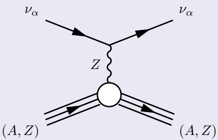

- Finally observed on CsI(2017) and LAr(2020)
  (other: MINER, TEXONO, CONNIE, Ricochet, νGEN, ν-cleus etc.)
- CONUS (hints)
- Very high experimental sensitivity (low detector threshold) is required

Electroweak precision tests
NSIs
Electromagnetic neutrinos
Sterile neutrinos
Lepton Unitarity Violation
Impact to dark matter searches
... *much more to expect*

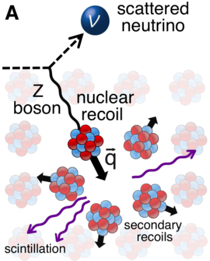

Thank you for your attention !

Extras

Experimental configuration

[Miranda, DKP, Tórtola, Valle, JHEP 1907 (2019) 103]

Experiment	detector	mass	threshold	efficiency	exposure	baseline (m)
			SNS			
COHERENT	CsI[Na]	14.57 kg [100 kg]	5 keV [1 keV]	Eq. (**??**) [100%]	308.1 days [10 yr]	19.3
COHERENT	HPGe	15 kg [100 kg]	5 keV [1 keV]	50% [100%]	308.1 days [10 yr]	22
COHERENT	LAr	1 ton [10 ton]	20 keV [10 keV]	50% [100%]	308.1 days [10 yr]	29
COHERENT	NaI[Tl]	2 ton [10 ton]	13 keV [5 keV]	50% [100%]	308.1 days [10 yr]	28
			Reactor			
CONUS	Ge	3.85 kg [100 kg]	100 eV	50% [100%]	1 yr [10 yr]	17
CONNIE	Si	1 kg [100 kg]	28 eV	50% [100%]	1 yr [10 yr]	30
MINER	2Ge:1Si	1 kg [100 kg]	100 eV	50% [100%]	1 yr [10 yr]	2
TEXONO	Ge	1 kg [100 kg]	100 eV	50% [100%]	1 yr [10 yr]	28
RED100	Xe	100 kg [100 kg]	500 eV	50% [100%]	1 yr [10 yr]	19

Calculation of the number of events above threshold

$$N_{\mathrm{theor}} = \sum_{\nu_\alpha} \sum_{x=\mathrm{isotope}} \mathcal{F}_x \int_{T_{\mathrm{th}}}^{T_A^{\mathrm{max}}} \int_{E_\nu^{\mathrm{min}}}^{E_\nu^{\mathrm{max}}} f_{\nu_\alpha}(E_\nu)\mathcal{A}(T_A) \left(\frac{d\sigma_x}{dT_A}(E_\nu, T_A)\right)_{\mathrm{tot}} dE_\nu dT_A \,,$$

- luminosity for a detector with target material x: $\mathcal{F}_x = N_{\mathrm{targ}}^x \Phi_\nu$
- $E_\nu^{\mathrm{min}} = \sqrt{m_A T_A/2}$: the minimum incident neutrino energy to produce a nuclear recoil

Statistical analysis

First phase of COHERENT (with a CsI detector)

$$\chi^2(\mathcal{S}) = \min_{\mathrm{a}_1,\mathrm{a}_2}\left[\frac{(N_{\rm meas} - N_{\rm theor}(\mathcal{S})[1+\mathrm{a}_1] - B_{0n}[1+\mathrm{a}_2])^2}{(\sigma_{\rm stat})^2} + \left(\frac{\mathrm{a}_1}{\sigma_{\mathrm{a}_1}}\right)^2 + \left(\frac{\mathrm{a}_2}{\sigma_{\mathrm{a}_2}}\right)^2\right].$$

- measured number of events is $N_{\rm meas} = 142$,
- a_1 and a_2 are the systematic uncertainties (signal and background rates), with $\sigma_{\mathrm{a}_1} = 0.28$ and $\sigma_{\mathrm{a}_2} = 0.25$.
- Statistical uncertainty $\sigma_{\rm stat} = \sqrt{N_{\rm meas} + B_{0n} + 2B_{ss}}$, where the quantities $B_{0n} = 6$ and $B_{ss} = 405$ denote the beam-on prompt neutron and the steady-state background events respectively.

Reactor experiments and next generation of COHERENT

$$\chi^2(\mathcal{S}) = \min_{\mathrm{a}}\left[\frac{(N_{\rm meas} - N_{\rm theor}(\mathcal{S})[1+\mathrm{a}])^2}{(1+\sigma_{\rm stat})N_{\rm meas}} + \left(\frac{\mathrm{a}}{\sigma_{\rm sys}}\right)^2\right],$$

- with $\sigma_{stat} = \sigma_{\rm sys} = 0.2$ (0.1) for the current (future) setups.

Probe TMMs through minimization over the nuisance parameter a and calculate $\Delta\chi^2(\mathcal{S}) = \chi^2(\mathcal{S}) - \chi^2_{\rm min}(\mathcal{S})$, with $\mathcal{S} \equiv \{|\Lambda_i|, \xi_i, \delta_{\rm CP}\}$

Constraints on TMMs from CEνNS experiments

Experiment	$\lvert\Lambda_1\rvert$	$\lvert\Lambda_2\rvert$	$\lvert\Lambda_3\rvert$
	SNS prompt		
CsI[Na]	69.2 [5.0]	70.2 [5.1]	89.6 [6.4]
HPGe	25.9 [5.1]	26.2 [5.2]	33.5 [6.6]
LAr	14.7 [2.9]	14.9 [2.9]	19.1 [3.7]
NaI[Tl]	16.6 [2.8]	16.8 [2.8]	21.5 [3.6]
	SNS delayed		
CsI[Na]	54.5 [4.2]	48.7 [3.7]	49.8 [3.7]
HPGe	21.3 [4.2]	18.9 [3.8]	19.1 [3.8]
LAr	11.3 [2.3]	10.1 [2.1]	10.4 [2.1]
NaI[Tl]	10.0 [2.3]	9.1 [2.0]	9.4 [2.0]
	Reactor		
CONUS	1.9 [0.37]	1.3 [0.26]	1.1 [0.22]
CONNIE	0.90 [0.13]	0.63 [0.09]	0.53 [0.08]
MINER	1.7 [0.58]	1.2 [0.41]	1.0 [0.34]
TEXONO	3.2 [0.46]	2.3 [0.32]	1.9 [0.27]
RED100	1.0 [0.14]	0.72 [0.10]	0.61 [0.08]
	Solar		
Borexino	0.44	0.36	0.28

90% C.L. limits on TMM elements $\lvert\Lambda_i\rvert$, in units of 10^{-10} μ_B, from current and future CEνNS experiments. The numbers in square brackets indicate the attainable sensitivities in the future setups.

- CEνNS experiments are sensitive to EM neutrino properties
- can probe TMMs at $10^{-11}\mu_B$ at least
- competitive with large-scale solar neutrino experiments

[Miranda, DKP, Tórtola, Valle, JHEP 1907 (2019) 103]

Exclusion curves to sterile neutrinos

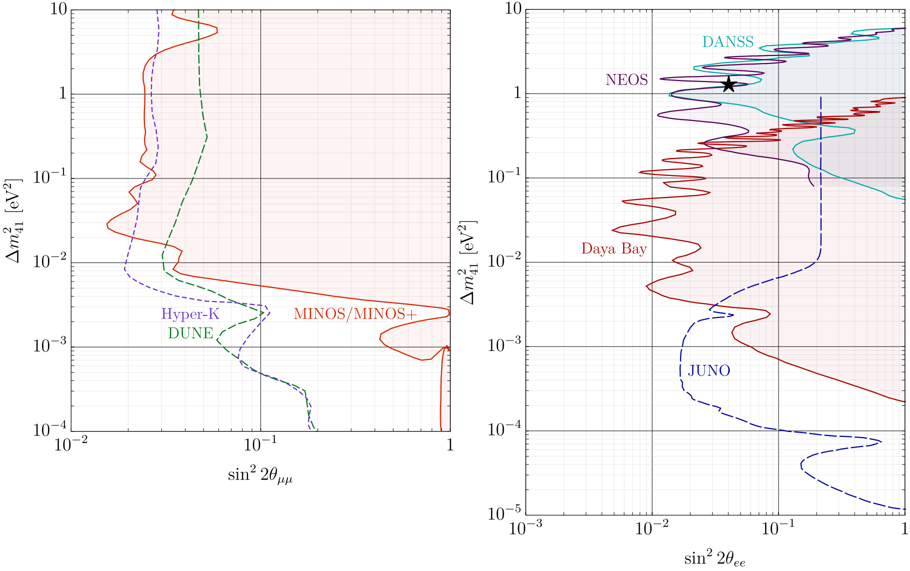

taken from

[Berryman PRD D100 (2019) 023540]